Ternary Alloys

Volume 21

MSI
Science Simplified

Ternary Alloys

A Comprehensive Compendium of Evaluated Constitutional Data and Phase Diagrams

critically evaluated by MSIT®

Volume 21

Selected Al-Fe-X Ternary Systems for Industrial Applications

Editors
Frank Stein, Martin Palm

Associate Editors
Liya Dreval, Oleksandr Dovbenko, Svitlana Iljenko

Authors
Materials Science International Team, MSIT®

MSI
Science Simplified

Editors: Frank Stein,
Martin Palm
Associate Editors: Liya Dreval
Oleksandr Dovbenko
Svitlana Iljenko

ISBN 978-3-932120-51-0

Vol. 21. Selected Al-Fe-X Ternary Systems for Industrial Applications. – 2022

This volume is part of the book series:
Ternary Alloys: A Comprehensive Compendium of Evaluated Constitutional Data and Phase Diagrams/
Materials Science International Services GmbH, Stuttgart, Germany

Group ISBN for the Ternary Alloys book series: 978-3-932120-41-1

Published by
MSI, Materials Science International Services GmbH, Stuttgart (Federal Republic of Germany)
Am Wallgraben 100, D-70565 Stuttgart, Germany
Postfach 800749, D-70507, Stuttgart, Germany
http://www.msiport.com
http://www.msi-eureka.com/

This book is subject to copyright. All rights reserved (including those of translation into other languages). No part of this book may be reproduced in any form – by photoprint, or any other means – nor transmitted or translated into a machine readable format without written permission from the copyright owner. Registered names, trademarks, etc. used in this book, even when not specifically marked as such, are not to be considered unprotected by law.

© Materials Science International Services GmbH, D-70565 Stuttgart (Federal Republic of Germany), 2022

This book was carefully produced. Nevertheless, authors, editors and publisher do not warrant the information contained therein to be free of errors. Readers are advised to keep in mind that statements, data, illustrations, procedural details or other items may inadvertently be inaccurate.

Printed on acid-free paper.

Printing and binding:
WIRmachenDRUCK GmbH, Mühlbachstraße 7, 71522 Backnang

Printed in the Federal Republic of Germany

Authors: Materials Science International Team, MSIT®

This volume results from collaborative evaluation programs performed by MSI and authored by MSIT®. In this program, data and knowledge are contributed by many individuals and have accumulated over almost thirty five years, up to the present day. The content of this volume is a subset of the ongoing MSIT® Evaluation Programs. Authors of this volume are:

Nataliya Bochvar, Moscow, Russia
Anatoliy Bondar, Kyiv, Ukraine
Gabriele Cacciamani, Genova, Italy
Lesley Cornish, Johannesburg, South Africa
Oleksandr Dovbenko, Stuttgart, Germany
Liya Dreval, Stuttgart, Germany
Yong Du, Changsha, China
Kiyaasha Dyal Ukabhai, Johannesburg, South Africa
Olga Fabrichnaya, Freiberg, Germany
Lorenzo Fenocchio, Genova, Italy
Sergio Gama, Campinas, Brasil
Gautam Ghosh, Evanston, USA
Bernd Grieb, Tübingen, Germany
Kiyohito Ishida, Sendai, Japan
Hermann A. Jehn, Stuttgart, Germany
Kostyantyn Korniyenko, Kyiv, Ukraine
Mario J. Kriegel, Freiberg, Germany
Ortrud Kubaschewski†, Aachen, Germany
K.C. Hari Kumar, Chennai, India
Bernard Legendre, Paris, France
Xiaojing Li, Changsha, China
Shuhong Liu, Changsha, China
Xing Jun Liu, Sendai, Japan
Annelies Malfliet, Heverlee, Belgium
Niraja Moharana, Chennai, India
Martin Palm, Düsseldorf, Germany
Jian Peng, Wuhan, China
Pierre Perrot, Lille, France
Alexander Pisch, Grenoble, France
Qingsheng Ran, Stuttgart, Germany
Maximilian Rank, Karlsruhe, Germany
Peter Rogl, Vienna, Austria
Lazar Rokhlin, Moscow, Russia
Rainer Schmid-Fetzer, Clausthal-Zellerfeld, Germany
Frank Stein, Düsseldorf, Germany
Vasyl Tomashyk, Kyiv, Ukraine
Lyudmila Tretyachenko†, Kyiv, Ukraine
Mikhail Turchanin, Kramatorsk, Ukraine
Oksana Tymoshenko, Kyiv, Ukraine
Thomas Vaubois, Chatillon, France
Alexander Walnsch, Freiberg, Germany
Chuanbin Wang, Wuhan, China
Cui Ping Wang, Sendai, Japan
Junjun Wang, Wuhan, China
Andrew Watson, Chesterfield, UK
Liming Zhang, München, Germany

Contents

Ternary Alloys
A Comprehensive Compendium of Evaluated Constitutional Data and Phase Diagrams

Volume 21
Selected Al-Fe-X Ternary Systems for Industrial Applications

Aluminium – Iron – Oxygen

Ortrud Kubaschewski†, Rainer Schmid-Fetzer, Lazar Rokhlin, Lesley Cornish, Olga Fabrichnaya

updated by Liya Dreval

Introduction

The system is important because alumina is used to reduce iron oxides in steelmaking, and knowledge of the slag properties, especially the effects of metal-slag reactions is essential for greater control in steelmaking [1953Gok, 1961Kuz, 1966Nov, 1975Kim, 1979Kay]. No complete phase diagram has been reported for the Al-Fe-O system, although specific reactions of mainly industrial interest have been investigated, especially the deoxidation of steel with Al and the sub-solidus reactions in the partial systems FeO-Al_2O_3-Fe_2O_3 and Al-Al_2O_3-Fe_2O_3-Fe [1954Ric, 1961Tur, 1962Tur, 1966Nov, 1980Mey, 1989Rag1, 1992Kub, 2007Kub].

The complex phase relationships in the Al-Fe-O system are partly due to the ratio of ferrous to ferric oxide at equilibrium, which itself is dependent on both temperature and oxygen pressure. The present critical evaluation updates the previous MSIT report written in 2007 by [2007Kub]. This survey describes the system by isothermal and polybaric projections. Among the many published contributions on the clarification and description of the phase relationships, only selected reports are given in the References section. The relation between deoxidation data and the phase equilibria is essential for understanding of discrepancies in this system, and will be elucidated in the *'Miscellaneous'* section. Table 1 summarizes the work done since 1994.

Binary Systems

The binary Al-O phase diagrams accepted from [1992Tay] are presented in Figs. 1a, 1b. Crystallographic data for solid phases are from [1985Wri]. The Al-Fe phase diagram is accepted from the binary evaluation report of [2022Ste] and presented in the chapter "*Al - Fe (Aluminium - Iron)*" of this volume. The phase diagrams of the Fe-O system are from the thermodynamic assessment of [1991Sun], while crystallographic data for high pressure and metastable/low temperature phases are from [Mas2], [V-C2], and [V-C]. The phase diagrams for the Fe-O system are presented in Figs. 2a and 2b.

Solid Phases

Data on the solid phases are given in Table 2. One ternary high temperature compound $FeAlO_3$ (τ), stable between 1318°C and about 1500°C, depending on the oxygen pressure was reported by [1956Mua, 1958Mua], although [2005Fee] synthesized the $FeAlO_3$ phase by heating a αAl_2O_3 + Fe_2O_3 mixture at 1300°C. Based on experimental data, formation of the $FeAlO_3$ was suggested at 1150°C [2001Lad].

$FeAl_2O_4$ (hercynite) and Fe_3O_4 (magnetite) form a continuous series of solid solutions at temperatures above 860°C [1962Tur]. At temperatures below 860°C, spinel has miscibility gap forming Fe rich and Al rich solid solutions.

Several studies (see section *'Quasibinary Systems'* and [2005Fee]) indicated restricted mutual solubility between αAl_2O_3 (corundum) and Fe_2O_3 (hematite). [1979Rou, 1991Skl], together with more recent investigations [2005Fee, 2005Liu], indicated formation of metastable extended γAl_2O_3 solid solution due to the distribution of Fe^{3+} ions in the γ modification of Al_2O_3. This solution is however unstable and tends to decompose into equilibrium phases upon prolonged heat treatment. It was shown in [2005Liu] that iron oxide doping reduced the γ to αAl_2O_3 transformation temperature.

Mechanical milling of mixtures consisting of various combinations of (Al), Fe_3O_4, Fe_2O_3 and Al_2O_3 extended the homogeneity ranges of some of the phases [2001Sur, 2003Bot, 2004Cot]. According to [2001Sur], during mechanical milling, Al_2O_3 dissolved up to 25 mol% Fe_2O_3.

Quasibinary Systems

The FeO-Al_2O_3 section was established as a quasibinary using DTA, X-ray, microscopy and petrographic analysis by [1966Nov]. Later version of the quasibinary system FeO-Al_2O_3 was proposed by [1974Ros]. However, it should be noted that the system is not strictly quasibinary because Fe occurs in different states of oxidation in varying amounts, even in oxide phases in contact with metallic Fe, and the "melting point" of FeO actually corresponds to a eutectic. However, experimental results are often represented in a way resembling a quasibinary diagram. The results are shown in Fig. 3 which summarizes findings of [1974Ros] and previous studies [1955Oel, 1956Fis] and [1957Gal],

and is in agreement with [1965Nov, 1966Nov]. The congruent melting point of $FeAl_2O_4$, reported by [1957Gal] as 1800°C, was accepted in Fig. 3 (1820, 1800 and 1820°C are given by [1956Fis, 1957Gal] and [1963Nov], respectively). X-ray diffraction and petrographic analysis of the samples from simultaneous sintering of iron aluminate and corundum at 1700°C showed that there is negligible miscibility between $FeAl_2O_4$ and αAl_2O_3 in the solid phase [1965Nov], which was later confirmed by [1974Ros]. According to earlier studies [1956Fis, 1956Mua, 1958Atl, 1964Roi], a measurable solution of αAl_2O_3 in $FeAl_2O_4$ occurs above 1350°C.

The Fe_3O_4-$FeAl_2O_4$ and Fe_2O_3-Al_2O_3 sections are also quasibinary, at least at temperatures below the solidus and high enough pressure to prevent oxide decomposition. [1962Tur] carried out experiments defining the limits of the spinel solid solution of the Fe_3O_4 (magnetite) - $FeAl_2O_4$ (hercynite) system. The buffered hydrothermal technique and lattice parameter measurements were used to find the solvus. A method of "bracketing" was developed, *i.e.* approaching the equilibria from both directions, the exsolution and solid solution. To induce solid solubility, samples were held for 2 d at 800°C, 12 d at 700°C and 1 month at 600°C, under a total pressure of 2 kbar. Equilibrium at 500°C was not obtained. The results are plotted in Fig. 4. Recently, [2020Agc] measured liquidus and solidus temperatures for a number of the samples related to the Fe_3O_4-$FeAl_2O_4$ section. The samples were produced in a reduction atmosphere. The reported data are to scarce to complement the partial vertical section (Fig. 4) reported by [1962Tur].

The Fe_2O_3-Al_2O_3 section below 1000°C was studied by [1962Tur] using their own data established by the hydrothermal method and X-ray analysis, combined with results published by [1956Mua,1958Atl] to construct the diagram in Fig. 5. Measurements by [1956Mua] were found to contain about 5 mass% less Al_2O_3 than those reported by [1958Atl] and extrapolated by [1962Tur].

More recent investigations by [1983Boj] indicate a lower solid solubility of αAl_2O_3 in Fe_2O_3 (Fig. 5). The solubility at lower temperatures has been determined by [1980Kli]. The $FeAlO_3$ compound appears at the upper limit of Fig. 5. Some "quasibinary" sections were calculated with a simple regular solution-type model as a basis for calculations in multicomponent oxide systems [1978Kau].

Invariant Equilibria

The reaction scheme for the Fe-Fe_2O_3-Al_2O_3-Al partial system, constructed by [1989Rag1], was corrected as described in the next section and is presented in Fig. 6. It includes the invariant points of the liquidus surface and incorporates the sub-solidus invariant reactions based on results published as isothermal sections. This scheme is simplified since it does not take the order-disorder transformation in the Al-Fe system into account.

The reaction p_1 at about 1700°C, $L_o + \alpha Al_2O_3 \rightleftharpoons Fe_2O_3$ (where L_o is oxide liquid) may also be of the eutectic type, $L'' \rightleftharpoons \alpha Al_2O_3 + Fe_2O_3$. This reaction must not be confused with the peritectic at about 1730°C shown later in the section Fe_2O_3-Al_2O_3 (Fig. 22) at 0.21 bar. This peritectic cannot appear in Fig. 6 since the entire reaction scheme is given under sufficient pressure to exclude the gas phase. An extrapolation of the Fe_2O_3 solvus and the αAl_2O_3 liquidus in Fig. 20 does not lead to a clear conclusion concerning the type of the reaction p_1.

The formation and decomposition of $FeAlO_3$ (τ) is also viewed differently compared to [1989Rag1]. The formation must occur above 1495°C as shown by the series of Figs. 19, 20 and 21, extrapolated to higher pressures. It is shown as P_1 in Fig. 6, an almost degenerated reaction with $FeAlO_3$ (τ) located almost on the tie-line Fe_2O_3-Al_2O_3. An alternative formation reaction in a three-phase maximum $Fe_2O_3 + \alpha Al_2O_3 \rightleftharpoons FeAlO_3$ is rather unlikely since it would require a larger O solubility range in Fe_2O_3 and αAl_2O_3 than in $FeAlO_3$. Thus, the three-phase invariant reactions given in [1989Rag1] at 1450 and 1318°C cannot be accepted. The decomposition of $FeAlO_3$ (τ) in E_3 at 1318°C (Fig. 6) is also almost degenerated and virtually identical to the 1318°C reaction in the Fe_2O_3-Al_2O_3 system at fixed oxygen partial pressure 0.21 and 1 bar, emphasizing the non-quasibinary character of these sections. Data on the invariant reactions at 1 bar total pressure involving Fe rich liquids are compiled in Table 3 [1972Ell].

The sequence of the phases in the U_4 reaction was changed comparing to [1989Rag1] and [2007Kub] to preserve the agreement with the preceding and subsequent ternary reactions. Some other misprints in phase denominations and temperatures in the reaction scheme reported by [2007Kub] were corrected in the present update.

The temperatures of U_7, U_8, U_9 were changed in the present work to preserve the constancy with the temperatures of the related invariant reactions in the Al-Fe system accepted here.

Liquidus Surface

[1989Rag1] proposed a schematic liquidus surface which may be mostly accepted. However, the liquid miscibility gap of the Al-O system had not been taken into account, suggesting that liquid Fe and liquid αAl_2O_3 form a continuous solution, which is extremely unlikely. Another proposition, given in Fig. 7, accepts a continuous band of

the miscibility gap between metallic liquid (L_m) and liquid oxides (L_o). As a consequence of this, the eutectic type reaction E_1'-E_1" and also a maximum e_2'-e_2" must occur. A critical point, given as c_1 and confused with the congruent melting point of $FeAl_2O_4$ by [1989Rag1], does not appear. Figure 7 incorporates the results of [1972Ell, 1979Ell]. The reactions e_3 and e_9 belong to the quasibinary system FeO-Al_2O_3 (Fig. 3). The invariant reactions U_6 to E_5 virtually coincide with the Al-Fe binary system. Quantitative data are available for liquidus surfaces in the Fe corner [1972Ell, 1979Ell]. Fig. 8 shows Fe rich part of the liquidus surface projection. The αAl_2O_3 liquidus surface has been studied by [1953Gok, 1954Ric, 1961Kuz, 1963Ent, 1965McL, 1967Swi, 1969Buz, 1969Nov, 1970Fru, 1971Roh, 1976Jan, 1981She, 1982Lia], the early solubility data of [1939Wen] are much too high (probably due to insufficient time being allowed for equilibrium) and have been disregarded.

Figure 9 gives isotherms of the αAl_2O_3 liquidus surface from the results reported by [1963Ent] for 1740 and 1910°C, [1967Swi] for 1580°C and [1981She] for 1600°C. The 1580°C and 1600°C isotherms also reflect the scatter of the data; the actual slope of the Al_2O_3 liquidus surface is considered to be smooth in the 1590 to 1910°C temperature range. [1963Ent, 1967Swi] investigated the Al and O contents of liquid Fe in equilibrium with Al_2O_3. [1963Ent] applied the gravimetric (Al_2O_3) and [1967Swi] the vacuum fusion method for the determination of the O concentration. As indicated by [1963Ent], the vacuum fusion method is susceptible to grave errors at high Al contents due to the absorption of gas by the Al distilled from the sample and the vaporization of Al_2O, which would account for the low oxygen contents at high Al concentrations in the 1580°C isotherm. The results of [1967Swi] appear to be inconsistent with other data, and thus, this may arise from his method of oxygen analysis. The findings agree that the solubility of O in Al-Fe melts decreases with increasing Al content to a minimum and then increases rapidly as shown in Fig. 9, 0.39 mass% Al decreases the solubility of oxygen in liquid Fe to a minimum of 8 ppm (0.0008 mass% O) at 1600°C.

The 0.01 to 100 mass% Al range at 1600°C was studied by [1981She] who also discussed earlier work by [1961Kuz]. The initial materials were hydrogen-refined carbonyl-iron and high purity Al. The solubility of oxygen was examined by the phase equilibrium method [1981She, 1970Nov]. The curve has two minima and one maximum. The first minimum is in good agreement with published data [1961Kuz, 1963Ent, 1967Swi, 1971Roh]. There are no other reported data on the position of the second minimum. The maximum approaches the experimental findings by [1963Ent] and [1970Fru].

Oxygen concentration in liquid iron being equilibrated with αAl_2O_3 and $FeAl_2O_4$ was determined in experiments of [1966McL, 1975Kim] at temperatures 1550-1750°C. Oxygen solubility results obtained by [1969Nov] at 1600°C by calculation and the vacuum fusion method are higher than those reported by [1981She]. Values at the minimum are 0.0035 mass% O [1969Nov] and 0.0008 mass% O [1981She], respectively.

It should be mentioned that the isotherm at 1600°C in Fig. 9 has been moved down within the experimental uncertainty, because the curve from the original work [1981She] intersected with the isotherm at 1740°C and it was far away from the isotherm at 1580°C while the temperature difference was only 20°C.

Isothermal Sections

[1961Tur, 1962Tur] studied Fe spinels by controlled synthesis from chemical mixtures in the temperature range 500 to 900°C and used X-ray measurements for the determination of solid solutions. Silver, which is not miscible with Fe at the temperature involved, was used as container material. Reaction rates were slow and experiments lasted up to 40 d. The isothermal sections displayed in Figs. 10 to 14 summarize the experimental results by [1961Tur, 1962Tur, 1980Mey] and [1983Elr], as well as findings from a review published by [1989Rag1] for the partial systems Fe-Fe_2O_3-Al_2O_3-Al and FeO-Fe_2O_3-Al_2O_3. The isothermal sections must be seen in conjunction with the oxygen pressure (stability) diagrams, given in the *'Potential Diagrams'* section, where the techniques used by [1980Mey] and [1983Elr] are also described.

Potential Diagrams

[1980Mey] determined the composition limits for the spinel solid solution $Fe_{3-x}Al_xO_4$ (σ) experimentally as a function of oxygen pressure at 1500, 1380 and 1280°C using lattice parameter measurements. The results were combined with information from the literature [1946Dar, 1956Fis, 1956Mua, 1958Atl, 1958Phi, 1964Roi, 1976Sti, 1976Pol] to develop self-consistent stability diagrams (Figs. 15 to 17), which show $p(O_2)$ *versus* cation (metal) fraction at constant temperatures for the Al-Fe-O system. In these diagrams, the left and right vertical axes constitute the binary Fe-O and Al-O systems, respectively. The complete spinel solid solution does not exist at any specific oxygen pressure. The spinels with higher Al content are only stable at lower oxygen pressure. The metallic Al-Fe phases would only appear in the very low-pressure range, which is not shown in Figs. 15 to 17.

[1983Elr] determined the equilibrium oxygen pressures of the univariant ternary equilibria of Fe_2O_3+$Fe_{3-x}Al_xO_4$+αAl_2O_3, metal+$Fe_{1-x}O$+$Fe_{3-x}Al_xO_4$ and metal+$Fe_{3-x}Al_xO_4$+αAl_2O_3, where the metal is essentially pure Fe. They used data derived from solid state electrochemical cell experiments in the temperature range 850 to 1150°C in combination with published data [1956Mua, 1958Mua, 1958Atl, 1962Tur, 1964Roi, 1981Pet] to construct oxygen pressure diagrams at 1000°C, 900°C and 800°C, as shown in Figs. 18 to 20, where the boundaries for the Al- or Fe-rich spinel are schematic. The spinel miscibility gap (Fe_3O_4+$FeAl_2O_4$) appears at 800°C in Fig. 20 and at 700°C in Fig. 12. The Fe_3O_4+$FeAl_2O_4$ boundaries are virtually independent of pressure. The composition of the spinel phase in equilibrium with αAl_2O_3 at 900°C and $p(O_2)$ = 10^{-12}, 10^{-13} and 10^{-14} bar was reported by [1962Tur]. $Fe_{1-x}O$ dissolves up to 0.55 mol% Al_2O_3. Alumina (αAl_2O_3) was found to dissolve approximately 1.1 at.% Fe in the temperature region 1000°C to 1300°C, whereas the Al content in the Al-Fe alloys was extremely small. The data of the Fe_3O_4/FeO equilibrium were taken from [1946Dar, 1969Bry]. [1984Sch] produced a projection of the aluminium and oxygen contents for FeO-Al_2O_3, as well as a polythermal deoxidation diagram of aluminium. However, these diagrams are not presented here, because they are inconsistent with the diagram of the FeO-Al_2O_3 system accepted in the present work. In a study of diffusion coatings, [2001Jha] plotted the relationship of oxygen potential and (low) Al content.

The effect of oxygen partial pressure on grain boundary migration in $95Al_2O_3{\cdot}5Fe_2O_3$ was studied by [1996Lee]. High oxygen partial pressure caused fast dissolution of the spinel, agreeing with earlier work described above, with migration of the Al_2O_3 solid solution grain boundaries. The Al_2O_3 was enriched in Fe_2O_3 after the boundary had passed. Low oxygen partial pressures gave grain boundary migration without spinel precipitation.

Temperature – Composition Sections

The Al_2O_3-Fe_2O_3 section was investigated at temperatures above 1000°C with different oxygen pressures by [1956Mua, 1958Mua]. They applied the “quenching method” and microscopy, as well as lattice parameter measurements for identification of different phases. $FeAlO_3$ (τ) exists in stable equilibrium only at temperatures above 1318°C and a partial pressure of O_2 above 0.03 bar. The upper decomposition temperature of τ is pressure dependent. The phase relationships are illustrated in Figs. 21 to 23 for decreasing oxygen pressure [1958Mua]. These vertical sections appear to be quasibinary diagrams, although this cannot be true at higher temperatures. The decomposition when heating pure Fe_2O_3 at 1390°C in Fig. 22 corresponds to the three-phase reaction: $6Fe_2O_3 \rightleftharpoons 4Fe_3O_4 + O_2$. The resulting spinel phase Fe_3O_4 is no longer located on the section Fe_2O_3-Al_2O_3 and this shift is balanced by substantial amounts of O_2 (gas), which is the meaning of the designation “+O_2” in the upper phase fields. A slight inconsistency concerns the reported solubility limits of the Fe_2O_3+$Fe_{3-x}Al_xO_4$ equilibrium. According to [1958Mua] (Figs. 21 to 23) the solubility of Al_2O_3 in $Fe_{3-x}Al_xO_4$ is larger than in Fe_2O_3. This is reversed in Figs. 16 to 20, however, where the solubility differences are small. The experimental data of [2009Rha] regarding the Fe_2O_3 solvus at a partial pressure of O_2 of 0.21 bar agree well with the corresponding data of [1954Ric, 1958Atl, 2001Lad]. [1992Tru] calculated the oxygen concentration in (γFe) in equilibrium with αAl_2O_3, $FeAl_2O_4$ and $Fe_{1-x}O$ (denoted ‘FeO’) as shown in Fig. 24.

Thermodynamics

In the literature, there is a great number of publications about equilibria in the Fe rich composition range. The data were obtained for the equilibrium between liquid iron and solid Al_2O_3 according to the reaction:

$$Al_2O_3(s) = 2\{\text{mass\% Al}\} + 3\{\text{mass\% O}\} \quad (1)$$

using the equilibration method with gas mixtures [1953Gok, 1961Kuz, 1963Ent, 1966Nov, 1967Swi, 1970Nov, 1970Sch, 1973Buz, 1981She, 1998Seo] and from emf measurements [1970Fru, 1976Jan, 1979Kay 1992Sui, 1995Dim]. The Gibbs energy of reaction (1) is given in Table 4 according to the recommendation of [2000Jan], based on analysis of experimental data on phase equilibria and emf measurements. The same methods were used to study equilibrium of iron liquid with $FeAl_2O_4$ (σ) and solid Al_2O_3 according to the reaction (2):

$$FeAl_2O_4(s) = Fe_L + Al_2O_3(s) + 1\{\text{mass\% O}\} \quad (2)$$

The Gibbs energy of reaction (2) was obtained by the equilibration technique [1960Pil, 1966McL, 1966Nov, 1975Kim] and emf [1963Rez, 1973Cha, 1973Jac, 1978Apt, 1978Sto, 1979Kay]. The results of [1978Apt] are in a good agreement with other data and they are recommended here (Table 4).

The experimental data for the spinel + solid Al_2O_3 + (γFe) equilibrium obtained by equilibration with a gas mixture and emf were analyzed by [1992Tru] for the Gibbs energy for the reaction:

$$(\gamma Fe) + 1/2O_2(gas) + Al_2O_3(s) = FeAl_2O_4(\sigma) \quad (3)$$

are recommended. The expression of Gibbs energy is presented in Table 4.

The results of experimental studies of the reaction (1) were thermodynamically treated and equilibrium constants and mixing parameters of liquid were derived. The oxygen and aluminum solubility in liquid were described by Wagner's model with first-order parameters by [1953Gok, 1961Kuz, 1963Ent, 1965Vac, 1967Buz, 1968Pie, 1970Fru, 1974Fel, 1976Jan], and with higher order parameters by [1974Sig, 1986Gho, 1992Hol, 1995Dim, 1995Jow, 1997Ito]. [1980Gus] presented two equations involving first order and higher order interaction parameters. The thermodynamic descriptions with first order parameters reproduce experimental data only for compositions up to 0.3 mass% Al. Involving higher order parameters makes it possible to reproduce experimental data up to 2 mass% Al. However, at higher concentrations of Al, the calculated oxygen content drastically decreases, which was not confirmed by experimental data. [1968Pie] suggested that taking the formation of the AlO cluster into account should improve fit to experimental data. In the calculation of the liquidus isotherms, [1982Lia] used the thermodynamic model based on Wagner's solvation-shell approach, which required data only from the binary edge systems. His predictions for the ternary Al-Fe-O liquid alloys are in good agreement with the experimental data and Fig. 9 up to about 3 mass% Al, while at 10 mass%, the calculated solubility at 1627 to 1727°C is approximately 0.1 mass% O, about 10 times higher than the data of [1981She] at 1600°C. [1981She] investigated Al-Fe alloys from 0.01 to 100 mass% Al, and indicated two minima (at 0.39 and 19.9 mass% Al) and one maximum (at 7.7 mass% Al) on oxygen solubility curve, using two different equations to describe his data in different composition ranges. It should be mentioned that similar shape of oxygen solubility was observed for Cr-Fe alloys [1968Pie]. In addition, [1982Lia] clearly demonstrated that previous calculations using interaction parameters are not suitable above 0.3 mass% Al. At higher Al contents, the first order interaction parameter calculation gives a too strong increase in O solubility. The calculation with both first and second order parameters also gives a maximum qualitatively similar to the one at 1600°C in Fig. 9, but at a much lower Al content of about 1 mass% Al and then the O solubility drops to unrealistic low values with only a slight increase of Al content. It can be also concluded that the interaction parameter type calculation must fail at higher Al contents since it is in principle restricted to "infinite" dilution of both O and Al, while the solvation-shell approach is in principle valid over the entire Al-Fe composition range. This calculation should be redone using the new experimental Al-O data of [1981She].

The solubility curves of $FeAl_2O_4$ have also been calculated by [1982Lia], and from the intersection with the Al_2O_3 liquidus isotherms it was concluded that $FeAl_2O_4$ is the most stable oxide precipitate in the liquid below $0.2 \cdot 10^{-4}$ mass% Al at 1627°C and $2.5 \cdot 10^{-4}$ mass% Al at 1827°C. The oxygen solubilities at the L+Al_2O_3+$FeAl_2O_4$ three-phase equilibrium are 0.053, 0.074, 0.1 and 0.134 mass% O at 1550, 1600, 1650 and 1700°C, respectively, and are in agreement with experimental data [1966McL, 1975Kim].

The associate model for metallic liquid was used by [1988Was, 1995Bou]. [1988Was] considered Fe_3Al, FeAl, $FeAl_3$, FeO, $FeAl_2O_4$, Al_2O_3 and Al_2O as associates. The shape of oxygen solubility curve obtained by [1988Was] was characterized by the presence of two minima in O content and in Al content. However, there is no experimental evidence of a minimum in Al content at low oxygen concentrations. [1995Bou] optimized thermodynamic parameters using three models: Wagner's formalism with high-order mixing parameters, an associate model accounting only for AlO species, and an associate model with both species AlO and Al_2O. [1995Bou] showed that the maximum in the oxygen solubility was apparently due to a large positive second order parameter in Wagner's formalism. The large and negative first-order interaction parameter indicates strong short-range interaction between oxygen and aluminum. When the AlO clusters were introduced into the model by [1995Bou], a good agreement between experimental and calculated values was obtained. The introduction of Al_2O species as well as AlO also reproduced experimental data satisfactorily. In the latter model, the liquid phase was virtually ideal; *i.e.* the excess Gibbs energy of solution is small.

The obtained thermodynamic data for reaction (2) in combination with other thermodynamic data makes it possible to calculate the enthalpy and entropy of formation of $FeAl_2O_4$ from solid Al_2O_3 and Fe [1992Tru]. There is a large scatter in both enthalpy of formation from elements and standard entropy values for the $FeAl_2O_4$ at 298.15 K [1988Ber, 1995Bar, 1993Kub, 1993Sax, 1990Hol, 1997Got, 2004Fab]. Some of these data [1990Hol, 1993Sax, 1997Got, 2004Fab] are results of optimizations based on high-pressure mineral reactions. The reason for inconsistencies can be the different degrees of cation disordering between octahedral and tetrahedral sites in the $FeAl_2O_4$. The degree of inversion was determined from neutron diffraction, and the results were treated by thermodynamic models [1998Har]. New adiabatic calorimetry measurements from 3 to 400 K have provided heat capacity data and a standard entropy value at room temperature [2003Kle], which are given in Table 5. The new entropy value is 7.6 $J \cdot (mol \cdot K)^{-1}$, which is higher than the previous adiabatic calorimetry result of [1956Kin], although the latter did not take the magnetic contribution to the entropy into account.

Activity measurements were conducted in oxygen-rich liquids in the Fe_3O_4-$FeAl_2O_4$ system [1969Sch, 1981Pet, 2011Lyk] and FeO-Al_2O_3 systems [1980Ban, 2004Fre], using a gas equilibrium technique. The activity in the

Fe_3O_4-$FeAl_2O_4$ system was investigated at 900°C and compositions up to 65 mol% Fe_3O_4 by [1969Sch], at 1300°C and compositions up to 80 mol% Fe_3O_4 by [1981Pet] and between 850 and 1000°C for the whole composition range by [2011Lyk]. In these studies, negative deviations from ideal behavior were indicated, although at high temperatures, deviation from ideality decreased. The experimental activities in the Fe_3O_4-$FeAl_2O_4$ system at 900°C and 1300°C are shown in Figs. 25 and 26. The activity of FeO was studied at 1400°C at compositions up to 8.9 at.% Al_2O_3 by [1980Ban], while in [2004Fre], data were obtained at 1550°C and 1600°C and compositions up to 14 at.% Al_2O_3. Both investigations demonstrated negative deviations from ideal behavior. It should be mentioned that the experimental data on activity in the FeO-Al_2O_3 system [2004Fre] demonstrate quite large scatter. The experimental data of [1980Ban, 2004Fre] were fitted using a liquid model from [2000Bjo] and interaction parameters were assessed. The fitted data on the FeO activity for the FeO-Al_2O_3 system at 1400 and 1600°C from [2004Fre] are presented in Fig. 27. Authors of [2004Fre] also made calculations of activities (a_{FeO} and a_{Al2O3}) in the FeO-Al_2O_3 system using an ionic liquid model and a modified quasi-chemical model of liquid and thermodynamic data available in Thermo-Calc and Fact-Sage databanks, respectively. Activity values in the FeO-Al_2O_3 liquid were also calculated by [2000Bjo] from experimental data of [1980Ban], using a model for liquid phase described in [2000Bjo]. As a demonstration, [2002Dav] calculated an isopleth between Fe_2O_3 and Al_2O_3 in air.

The enthalpy of formation of the Fe_2O_3-Al_2O_3 solid solution was determined by drop-solution calorimetry by [2002Maj]. The temperature dependent mixing parameter was assessed in [2002Maj] to reproduce solvus data. The more complicated asymmetric model with temperature dependent parameters was applied by [2005Fee] to describe excess Gibbs energy of the Fe_2O_3-Al_2O_3 solid solutions using available data on miscibility gap and calorimetric data of [2002Maj]. The enthalpy of mixing is presented in Fig. 28. For the $FeAlO_3$ compound, the enthalpy of formation from oxides and heat capacity were determined by drop-solution calorimetry, and by differential scanning calorimetry by [2002Maj], with the data presented in Tables 4-5. The standard entropy of the $FeAlO_3$ was calculated by [2002Maj] taking into account vibrational, magnetic, dilatational and configurational contributions due to disordering contributions as 98.9 $J\cdot(mol\cdot K)^{-1}$.

An assessment of thermodynamic functions was presented by [1978Kau]. The calculated phase diagrams of Fe_3O_4-Al_2O_3, FeO-Al_2O_3, Fe_2O_3-Al_2O_3 are in a reasonable agreement with experimental data. The phase diagram of the FeO-Al_2O_3 system was calculated using thermodynamic data of [1984Sch, 1993Eri]. The diagram of [1993Eri] was calculated using a quasi-chemical model for liquid. It should be mentioned that the character of $FeAl_2O_4$ (σ) melting is peritectic and this contradicts experimental data of [1956Fis, 1966Nov, 1974Ros], *i.e.* the peritectic melting of the $FeAl_2O_4$ indicated by [1955Oel] was not confirmed by later studies. The activities of FeO and $AlO_{1.5}$ in the liquid phase were calculated at 1900 and 2200°C by [1993Eri], with positive deviations from ideal behavior at both temperatures. Since experimental data did not show strong temperature dependence, it is likely that the description of [1993Eri] is in contradiction with the FeO experimental activity data of [1980Ban, 2004Fre]. The 3-D potential diagram of the Al-Fe-O system, based on thermodynamic calculations of [1999Yok], is presented in Fig. 29, with the formation of the Fe_3O_4-$FeAl_2O_4$ spinel solid solution taken into account (calculations without this consideration is shown by a dashed line).

Between 2015 and 2016, three thermodynamic assessments of this system appeared in the literature. [2015Lin, 2016Dre, 2018Dre] are mainly focused on the oxide part of the system. [2016Shi] also included the thermodynamic models of the Al-Fe compounds in their assessment. However, not relevant parameters were evaluated for the Al-Fe phases because of the lack of the experimental data. [2016Shi] also used the simplified sublattice models for $FeAl_2$ and Fe_2Al_3 which do not take the homogeneity ranges of these compounds into account. Thus, the results of [2016Shi] for the metallic part should be considered as a mere prediction.

Notes on Materials Properties and Applications

The alloys of the Al-Fe-O system are interesting as materials in applications requiring high resistance to oxidation and sulfidation. The alloys consist of an Fe-40 at.% Al matrix with embedded Al_2O_3 particles, where the Al_2O_3 particles improve the high temperature strength of the alloys (composites) [1997Sub, 2003Lan, 2003Mun]. One of the ways to prepare such alloys is a pre-oxidation of the Fe-40 at.% Al alloy in air, where the gas corrosion resistant layer of the Al-Fe-O alloy is formed on a designated surface [2003Lan]. In [2001Mas], microstructure and oxidation behavior of Fe-40 at.% Al layers deposited on iron plate by low-pressure plasma spraying method were studied and good resistance to oxidation of the layers at high temperatures was confirmed. Al-Fe-O alloys also have interesting magnetic and thermopower properties [2002Gra, 2003Xue]. In [2002Gra], tunneling thermopower in the Al-Fe-O alloys was studied. In nano-composite Al_2O_3-Fe_2O_3, the phenomenon of superparamagnetism was revealed by [2005Liu].

[1985Tay] presented characteristics of thermal expansion of $FeAl_2O_4$ (hercynite). [1983Yam] investigated vacancy diffusion in the Fe_3O_4-$FeAl_2O_4$ solid solution. [1971Iml] measured microhardness of the spinel Fe_3O_4-$FeAl_2O_4$ solid solution, showing a linear relationship between 675 for magnetite to 1550 for hercynite. [2004Vil] measured the magnetic susceptibility of $Fe_{2-x}Al_xO_3$ compound.

Miscellaneous

The Al-Fe-O phase diagram is applied widely in the analysis and understanding of various metallurgical processes, such as the deoxidation of molten steel by addition of Al. During deoxidizing, Al_2O_3 particles are formed in the melt and tend to escape. In [2000Jan, 2001Sas], the behavior of the Al_2O_3 particles in the deoxidizing steel during continuous casting was investigated, by considering the phase equilibria in the Al-Fe-O system. [1991Nak, 2003Kap] studied wettability of Al_2O_3 by liquid iron with different oxygen contents. [2002Was] applied thermodynamic analysis to study Al_2O_3 formation in deoxidized iron. [1985Meh] used interaction data between molten Fe and solid Al_2O_3 for the development of a model to predict the interfacial behavior in ceramic-molten metal systems with varying partial pressure of oxygen. In [1999Mei], the Al-Fe-O phase diagram was used for analysis of the wide-spread thermite reaction between Fe_2O_3 and Al.

[2002Bot, 2003Bot] studied the reaction in a Al-Fe_3O_4 mixture activated by ball milling. The reaction was ended by formation of the (αFe), $FeAl_2O_4$ and Al_2O_3 phases, which conformed to the equilibrium Al-Fe-O phase diagram. The particular phases formed after the reaction depended on the ratio between components in the mixture Al-Fe_3O_4 [2001Sur].

[2002Tak] reported attempts to prepare magnetic nano-composites consisting of Fe and Al_2O_3 phases by mechanically induced self-propagating reactions in the Fe_3O_4-Al mixture. However, the product obtained after combustion contained significant contents of $FeAl_2O_4$, as well as the targeted Fe and Al_2O_3 phases. Similar results were obtained by [2002Tak], when hematite Fe_2O_3 was reduced with Al by the same method of mechanically induced self-propagating combustion.

Experiments by [1999Fuj] on the deoxidation equilibrium for aluminum in liquid iron and an Fe-36%Ni alloy under pressure controlled by H_2/H_2O gas at 1700°C resulted in the interaction parameters between Al and O in liquid iron and the Fe-36%Ni alloy. [1990Kuz] studied the effect of alloying with Zr, Al-Zr, Hf and Al-Hf on oxygen activity in Co-Cu-Fe-Ni alloys at 1600°C.

[1999Yok] discussed features of generalized chemical potential diagrams and their application to interface reactions between materials having different chemical bonds, such as alloys and ceramics. The calculated stability diagram of the Al-Fe-O system as a function of chemical potentials was presented as an example of a system including solid solutions. A stability diagram for the Al-Cr-Fe system as function of oxygen and sulfur partial pressure at 982°C was calculated by [1979Gor] and utilized to estimate corrosion resistance of alloys used in natural gas production. [1993Tyu] presented thermodynamic descriptions of systems involving an Fe-containing alloy, oxide solid solutions and oxide-sulfide melt.

[2002Gos] reported hematite (Fe_2O_3) produced *via* oxinate precursors by combustion at 700°C in an air flow to incorporate up to 10 at.% Al. Oxidation of an alloy Fe-2 mass% Al was accompanied by formation of a thin Al_2O_3 film on its surface if the oxygen pressure was less than 10^{-7} torr, and by the Fe_3O_4 film on the surface with the layer of Al_2O_3 underneath, if the oxygen pressure was higher than 10^{-7} torr [1980Aki].

[1979Nec] studied the solubility of Fe in (Al), and materials with high density of dislocations stabilized by Al_2O_3 by Mössbauer spectroscopy. [1984Mac] synthesized the ternary compound $FeAlO_3$ ($Fe_{2-x}Al_xO_3$) at 1370°C, and studied its room-temperature Mössbauer spectrum. Analysis of the spectrum suggested that Fe^{3+} ions occupied both tetrahedral and octahedral sites in the compound lattice. [1998Cos] reviewed and conducted their own study on the Mössbauer spectra of maghemite (γFe_2O_3) and aluminium-substituted maghemite ($\gamma(Fe_{1-y}Al_y)_2O_3$). The dependence of the Mössbauer spectra of the compounds on formation conditions and the possible sites of the ions in their lattices were discussed.

[1990Tsu] studied the solid solution formation between Fe_2O_3 and Al_2O_3 during annealing of mixtures of goethite (αFeOOH) with various hydrated aluminas. Preliminary grinding of the mixtures was established to accelerate the reactions. [1991Yao] investigated the behavior of spinel $FeAl_2O_4$ during annealing at 1200°C under low oxygen partial pressure ($7.1\cdot10^{-11}$ - $1.4\cdot10^{-8}$ Pa). With increasing annealing time, the spinel decomposed partially forming metallic Fe and αAl_2O_3. Decreasing oxygen partial pressure accelerated the decomposition. X-ray investigations indicated a decrease in the $FeAl_2O_4$ lattice parameter after partial decomposition, which was explained by vacancy formation in lattice sites of the escaped Fe ions. Mössbauer spectra indicated that the ratio of the Fe ions in the

tetrahedral sites compared to the total number of Fe ions in the $FeAl_2O_4$ lattice decreased in the decomposition process.

Al is the strongest deoxidiser commonly used in steelmaking. The extent to which it removes dissolved oxygen has been the subject of many investigations. After the work of [1953Gok], it is known that the "deoxidation constant" is extremely small. The equilibrium constant for the reaction $Al_2O_3(s) \rightleftharpoons 2\{Al\}_{Fe} + 3\{O\}_{Fe}$ can be calculated. However, it disagrees with the bulk of the deoxidation constants observed in practice [1979Kub]. The reason for this discrepancy appears to be the following: firstly, when the Al shot is added to undeoxidized liquid steel, the reaction of the solid Al particle with {O} in the immediate surroundings to form Al_2O_3, proceeds at a higher rate than that at which Al dissolves and diffuses through the Fe. Secondly, the resultant Al_2O_3 particle in a deoxidized area is transmitted to an undeoxidized region by turbulences. Oxygen in the undeoxidized area comes out of solution to form FeO, which in turn combines with the Al_2O_3 particle to form the spinel $FeO{\cdot}Al_2O_3$ ($FeAl_2O_4$). This would result in a high FeO content, as well as a larger deoxidation constant [1957Fit]. Careful experiments over longer time periods proved that the deoxidation constant varies with time. [1967Rep, 1973Iye] demonstrated that projecting the path of reactions with the aid of the phase diagram, allows the metastable or non-equilibrium conditions to be predicted.

The change of Mössbauer spectra, magnetic properties and reduction rate of magnetite-based solid solutions were studied as function of impurity additions of Al, Ca and Mg [1976Mal].

The "quasibinary" system FeO_4-Al_2O_3 has been calculated by [1984Sch] in stable, as well as metastable versions, in which the formation of $FeAl_2O_4$ is suppressed. The results of the calculation are in agreement with the experiments of [1955Oel, 1956Fis].

References

[1939Wen] Wentrup, H., Hieber, G., "Reactions Between Al and O in Iron Melts", *Arch. Eisenhuettenwes.*, **13**, 15-20 (1939), doi:10.1002/srin.193900854 (Phase Relations, Experimental, 10)

[1946Dar] Darken, L.S., Gurry, R.W., "The System Iron-Oxygen: II", *J. Am. Chem. Soc.*, **68**, 798-816 (1946), doi:10.1021/ja01224a050 (Phase Relations, Phase Diagram, Experimental, Thermodynamics, 24)

[1953Gok] Gokcen, N.A., Chipman, J., "Aluminium-Oxygen Equilibrium in Liquid Iron", *Trans. AIME*, **5**(2), 173-178 (1953) (Phase Relations, Phase Diagram, Experimental, Thermodynamics, 12)

[1954Ric] Richards, R.G., White, J., "Phase Relationships of Iron-Oxide-Containing Spinels. Part I. Relationships in the System Fe-Al-O", *Trans. Brit. Ceram. Soc.*, **53**, 233-270 (1954) (Experimental, Phase Diagram, Phase Relations, 26)

[1955Oel] Oelsen, W., Heynert, G., "The Reaction Between Iron-Manganese Melts and Melting of their Aluminate" (in German), *Arch. Eisenhuettenwes.*, **26**(10), 567-575 (1955), doi:10.1002/srin.195502081 (Phase Relations, Phase Diagram, Experimental, 12)

[1956Fis] Fischer, W.A., Hoffmann, A., "The Phase Diagram Ferrous Oxide - Aluminium Oxide" (in German), *Arch. Eisenhuettenwes.*, **27**(5), 343-346 (1956) (Experimental, Phase Diagram, 15)

[1956Kin] King, E.G., "Heat Capacities at Low Temperatures and Entropies of Five Spinel Minerals", *J. Phys. Chem.*, **60**, 410-412 (1956), doi:10.1021/j150538a006 (Experimental, Thermodynamics, 17)

[1956Mua] Muan, A., Gee, C.L., "Phase Equilibrium Studies in the System Iron Oxide-Alumina in Air and at One Atmosphere Oxygen Pressure", *J. Am. Ceram. Soc.*, **39**, 207-214 (1956), doi:10.1111/j.1151-2916.1956.tb15647.x (Experimental, Phase Diagram, Phase Relations, 17)

[1957Fit] Fitterer, G.R., "The Physical Chemistry of Steelmaking - A Tribute to Dr. C. H. Herty, Jr.", *Proc. 40th Nat. Open Hearth Steel Comm. Iron Steel Division, AIME,* Pittsburgh, **40**, 281-303 (1957) (Experimental, Phase Relations, Physical Properties, 40)

[1957Gal] Galakhov, F.Ya., "Alumina Regions of Ternary Aluminosilicate Systems. Communication 1. The Systems FeO-Al_2O_3-SiO_2 and MnO-Al_2O_3-SiO_2" (in Russian), *Izv. Akad. Nauk SSSR, Otd. Khim. Nauk*, **5**, 525-531 (1957), translated to *Bull. Acad. Sci. USSR, Div. Chem. Sci. (Engl. Transl.)*, **6**(5), 539-545 (1957), doi:10.1007/BF01169268 (Phase Relations, Phase Diagram, Experimental, 16)

[1958Atl] Atlas, L.M., Sumida, W.K., "Solidus, Subsolidus and Subdissociation Phase Equilibria in the System Fe-Al-O", *J. Am. Ceram. Soc.*, **41**(5), 150-160 (1958), doi:10.1111/J.1151-2916.1958.TB13532.X (Experimental, Phase Diagram, Phase Relations, 23)

[1958Mua] Muan, A., "On the Stability of the Phase $Fe_2O_3.Al_2O_3$", *Amer. J. Sci.*, **256**(6), 413-422 (1958), doi:10.2475/ajs.256.6.413 (Phase Relations, Phase Diagram, Experimental, #, *, 8)

[1958Phi] Phillips, B., Muan, A., "Phase Equilibria in the System CaO - Iron Oxide in Air and at 1 Atm. O_2 Pressure", *J. Am. Ceram. Soc.*, **41**(11), 445-454 (1958), doi:10.1111/j.1151-2916.1958.tb12893.x (Experimental, Phase Diagram, Phase Relations, 16)

[1958Tay] Taylor, A., Jones, R.M., "Constitution and Magnetic Properties of Iron-Rich Iron-Aluminium Alloys", *J. Phys. Chem. Solids*, **6**(1), 16-37 (1958), doi:10.1016/0022-3697(58)90213-0 (Crystal Structure, Experimental, Magnetic Properties, Phase Diagram, 49)

[1960Pil] Pillay, T.C.M., D'Entremont, J., Chipman, J., "Stability of Hercynite at High Temperature", *J. Amer. Ceram. Soc*., **43**(11), 583-585 (1960), doi:10.1111/J.1151-2916.1960.TB13620.X (Experimental, Thermodynamics, 9)

[1961Kuz] Kuznetsov, V.M., Samarin, A.M., "Deoxidation Capacity of Al in Liquid Iron" (in Russian), *Physiochemical Fundamentals of Steelmaking,* Izd. AN SSSR, Moscow, 11-17 (1961) (Thermodynamics, Phase Relations, Phase Diagram, Experimental, 8)

[1961Tur] Turnock, A.C., Lindsley, D.H., "Fe-Al and Fe-Ti Spinels and Related Oxides", *Carnegie Inst. Yearbook*, Washington, **60**, 152-157 (1961) (Phase Relations, Phase Diagram, Experimental, #, *, 3)

[1962Tur] Turnock, A.C., Eugster, H.P., "Fe-Al Oxides: Phase Relationships Below 1000°C", *J. Petrology*, **3**(3), 533-565 (1962), doi:10.1093/petrology/3.3.533 (Experimental, Phase Diagram, 35)

[1963Ent] d'Entremont, J.C., Guernsey, D.L., Chipman, J., "Aluminium - Oxygen Interaction in Liquid Iron", *Trans. Met. Soc. AIME*, **227**, 14-17 (1963) (Experimental, Phase Relations, 13)

[1963Nov] Novokhatskii, I.A., Lenov, L.M., *Izv. Akad. Nauk SSSR, Metall. i Gorn. Delo*, (6), 47 (1963) as quoted by [1965Nov]

[1963Rez] Rezukhina, T.N., Levitskii, V.A., Ozhegov, P., "Thermodynamic Properties of Iron Aluminate", *Russ. J. Phys. Chem*., **37**, 358 (1963) (Experimental, Thermodynamics, 11)

[1964Roi] Roiter, B.D., "Phase Equilibria in the Spinel Region of the System FeO-Fe_2O_3-Al_2O_3", *J. Am. Ceram. Soc.*, **47**(10), 509-511 (1964), doi:10.1111/j.1151-2916.1964.tb13799.x (Experimental, Phase Diagram, Phase Relations, 9)

[1965McL] McLean, A., Bell, H.B., "Experimental Study of the Reaction $Al_2O_3+H_2 \rightleftharpoons 3H_2O+2\underline{Al}$", *J. Iron Steel Inst.*, **203**, 123-130 (1965) (Experimental, Phase Relations, 33)

[1965Nov] Novokhatskii, I.A., Belov, B.F., Gorokh, A.V., Savinskaya, A.A., "The Phase Diagram for the System Ferrous Oxide-Alumina", *Russ. J. Phys. Chem.*, **39**(11), 1498-1499 (1965) (Phase Relations, Phase Diagram, Experimental, 9)

[1965Vac] Vachet, V., Desre, P., Bonnier, E., "Thermodynamics of the Liquid Systems (Fe, Al, O), (Co, Al, O), (Ni, Al, O) in the Fe, Co or Ni-Rich Regions at 1600°C" (in French), *Compt. Rend. Acad. Sci. Paris*, **260**(7), 1943-1946 (1965) (Experimental, Thermodynamics, 4)

[1966McL] McLean, A., Ward, R.G., "Thermodynamics of Hercynite Formation", *J. Iron Steel Inst.*, **204**, 8-11 (1966) (Experimental, Thermodynamics, 36)

[1966Nov] Novokhatsky, I.A., Belov, B.F., "Phase Equilibria and Distribution of Elements in the Fe-O-Al System" (in Russian), *Izv. Akad. Nauk SSSR, Met.*, (1), 38-48 (1966) (Phase Relations, Phase Diagram, Experimental, 18)

[1967Buz] Buzek, Z., Schindlerova, V., Macoszek, M., "The Influence of Cr, Mn, V, Si, Ti, Al, Zr, Ce and Ca on the Activity and Solubility of Oxygen in Liquid Iron", *Sb. Ved. Pr. Vys. Sk. Ban. Ost., Rada Hutn.*, **13**(2-3), 175-193 (1967) (Experimental, Phase Relations, 26)

[1967Rep] Repetylo, O., Olette, M., Kozakevitch, P., "Deoxidation of Liquid Steel with Aluminum and Elimination of the Resulting Alumina", *J. Metals*, 45-49 (1967) (Experimental, Phase Relations, 24)

[1967Swi] Swisher, J.H., "Note on the Aluminum-Oxygen Interaction in Liquid Iron", *Trans. Met. Soc. AIME*, **239**, 123-124 (1967) (Experimental, Phase Relations, #, 8)

[1968Pie] Pierre, G.R.St., Blackburn, R.D., "The Relationship Between First-Order Interactions and Oxide Solubilities in Liquid Iron", *Trans. Metall. Soc. AIME*, **242**, 2-4 (1968) (Experimental, Theory, 18)

[1969Bry] Bryant, P.E.C., Smeltzer, W.W., "The Dissociation Pressure of Hematite", *J. Electrochem. Soc*., **116**, 1409-1410 (1969) (Experimental, Phase Relations, 4)

[1969Buz] Buzek, Z., Hutla, A., "The Influence of the Aluminium, Titanium, Zirconium Dissolved in Liquid Iron on the Activity and Solubility of Oxygen" (in German), *Freib. Forsch. B*, *Metall. Werkstofftech*., **B117**, 59-73 (1969) (Experimental, Phase Relations, Phase Diagram, 20)

[1969Nov] Novokhatsky, I.A., Belov, B.F., "Concentration Dependence of the Solubility of Oxygen in Alloys" (in Russian), *Izv. Akad. Nauk SSSR, Met.*, (3), 15-26 (1969) (Phase Relations, Phase Diagram, Experimental, Thermodynamics, 29)

[1969Sch] Schmahl, G., Dillenburg, H., "Equilibrium Studies of Iron Oxide Containing Solid Solutions in the Ternary Systems Fe-Al-O, Fe-Cr-O and Fe-V-O" (in German), *Z. Phys. Chem.*, **65**, 119-138 (1969), doi:10.1524/zpch.1969.65.1_4.119 (Experimental, Phase Diagram, Phase Relations, 70)

[1970Fru] Fruehan, R.J., "Activities in Liquid Fe-Al-O and Fe-Ti-O Alloys", *Metall. Trans.*, **1**, 3403-3410 (1970), doi:10.1007/BF03037871 (Phase Relations, Experimental, Thermodynamics, 28)

[1970Nov] Novokhatskii, I.A., Belov, B.F., "Method for the Investigation of Reduction Processes of Metallic Melts", *Russ. J. Phys. Chem.*, **44**(8), 1138-1140 (1970), translated from *Zh. Fiz. Khim.*, **44**(8), 2013-2017, 1970 (Experimental, Phase Relations, 18)

[1970Sch] Schenck, H., Steinmet, E., Mehta, K.K., "Equilibrium and Kinetics of Precipitation of Alumina in System Iron-Oxygen-Aluminium at 1600°C" (in German), *Arch. Eisenhuettenwes.*, **41**(2), 131-138 (1970) (Experimental, Phase Relations, Thermodynamics, 51)

[1971Iml] Imlach, J.A., Glasser, F.P., "Sub-Solidus Phase Relations in the System CaO-Al_2O_3-Fe-Fe_2O_3", *Trans. J. Br. Ceram. Soc.*, **70**, 227-234 (1971) (Experimental, Phase Diagram, 7)

[1971Roh] Rohde, L.E., Choudhury, A., Wahlster, M., "New Investigation into the Aluminium-Oxygen Equilibrium in Iron Melts" (in German), *Arch. Eisenhuettenwes.*, **B42**(3), 165-174 (1971) (Phase Relations, Phase Diagram, Experimental, 50)

[1972Ell] Elliott, J.F., Wright, J.K., "Equilibrium Phase Relations During Solidification of Fe-O-C-X Alloys. System Fe-Al-O. Projected Equilibria Involving Iron Between 1500 and 1538°C at One Atmosphere", *Canad. Metall. Quart.*, **11**(4), 573-584 (1972), doi:10.1179/cmq.1972.11.4.573 (Phase Relations, Phase Diagram, Experimental, #, *, 17)

[1973Buz] Buzek, Z., "Effect of Alloying Elements on the Solubility and Activity of Oxygen and Sulphur in Liquid Iron at 1600°C", *Int. Symp. Metall. Chem. - Appl. Ferrous Metall.,* Sheffield, July 1971, Iron and Steel Inst, London, 173-177 (1973) (Crystal Structure, Experimental, Review, 8)

[1973Cha] Chan, J.C., Alcock, C.B., Jacob, K.T., "Electrochemical Measurement of the Oxygen Potential of the System Iron-Alumina-Hercynite in the Temperature Rang 750 to 1600°C", *Can. Metall. Quart.*, **12**(4), 439-443 (1973), doi:10.1179/cmq.1973.12.4.439 (Experimental, Thermodynamics, 15)

[1973Iye] Iyengar, R.K., Philbrook, W.O., "Application of Phase Diagrams to Predict Phases Formed During Deoxidation of Steel", *Metall. Trans.*, **4**(9), 2189-2193 (1973) (Phase Diagram, Experimental, 20)

[1973Jac] Jacquemot, A., Gatellier, C., Olette, M., "Study of Aluminium-Oxygen Equilibrium in Molten Iron at 1600°C with Help of Battery Having Solid Electrolyte ThO_2-Y_2O_3" (in French), *Compt. Rend. Acad. Sci. Paris, Ser. C*, **277**(6), C271-C273 (1973) (Experimental, Thermodynamics, 10)

[1974Fel] Feldman, S.E., Kirkaldy, J.S., "On the Solubility Minimum in Ternary Oxide-Metal Equilibria", *Canad. Metall. Quart.*, **13**(4), 625-630 (1974) (Theory, Phase Relations, 20)

[1974Ros] Rosenbach, K., Schmitz, J.A., "Investigations in the Ternary System Iron(II)-Oxide-Chromium(III)-Oxide-Alumina" (in German), *Arch. Eisenhuettenwes.*, **45**(12), 843-847 (1974), doi:10.1002/srin.197403968 (Phase Relations, Phase Diagram, Experimental, #, 13)

[1974Sig] Sigworth, G.K., Elliott, J.F., "The Thermodynamics of Liquid Dilute Iron Alloys", *Met. Sci.*, **8**, 298-309 (1974) (Review, Thermodynamics, 249)

[1975Kim] Kim, C.K., McLean, A., "Hercynite Formation in Molten Iron Alloys", in "*Metal-Slag-Gas Reactions and Processes*", Foroulis, Z.A., Smeltzer, W.W., (Eds.), Electrochem. Soc., Princeton, New Jersey, 284-295 (1975) (Phase Relations, Phase Diagram, Thermodynamics, Experimental, 12)

[1976Jan] Janke, D., Fischer, W.A., "Deoxidation Equilibria of Ti, Al and Zr in Fe Melts at 1600°C" (in German), *Arch. Eisenhuettenwes.*, **47**(4), 195-198 (1976), doi:10.1002/srin.197603805 (Experimental, Phase Relations, Phase Diagram, 30)

[1976Mal] Malysheva, T.Ya., Lyadova, V.Ya., Ostroskaya, I.V., Model, M.S., Davidyuk, A.A., "Nature of the Ferrite Phases in the Blast-Furnace Charge" (in Russian), *I. P. Bardin Razvit. Metall. SSSR*, Savitskii, E.M., (Ed.), Nauka, Moscow, 39-58 (1976) (Experimental, Phase Relations, 32)

[1976Pol] Pollak, T.M., "High Temperature Electrical Conductivity and Defect Chemistry of Iron-Doped Alumina", *Thesis*, Massachusets Inst. Technology, 81pp. (1976) (Electrical Properties, Experimental, 29)

[1976Sti] Sticher, J., Schmalzried, H., Schmalzried, C.-Z., "Geometrical Representation of Thermodynamic State Variables in the Ternary System Iron-Titanium-Oxygen in the Temperature Range Between 1300 and 1600°C" (in German), *Arch. Eisenhuettenwes.*, **47**(5), 261-266 (1976) (Theory, Thermodynamics, Phase Relations, Phase Diagram, Experimental, 54)

[1978Apt] Apte, P., Stournaras, C., Kay, D.A.R., "Steelmaking Thermodynamics and Oxygen Concentration Cells", *Conf. Steelmaking Proc.,* Chicago, Ill, 16-20 Apr. 1978, Amer. Inst. Min., Met. Petroleum Engin., **61**, 555-560 (1978) (Experimental, Phase Relations, 18)

[1978Kau] Kaufman, L., Nesor, H., "Calculation of Quasibinary and Quasiternary Oxide Systems - I", *Calphad*, **2**, 35-53 (1978) (Thermodynamics, Phase Relations, Phase Diagram, Theory, 30)

[1978Sto] Stournaras, C.J., "Thermodynamic Studies in Liquid Fe-Nb-O, Fe-Al-O, Fe-Al-Mn-O Systems Using Solid Electrolytes", *Diss. Absr. Int. B*, **38**(7), 3351 (1978) (Experimental, Thermodynamics, 0)

[1979Ell] Elliott, J.F., "Chemical Equilibria and Phase Equilibria", *TMS / AIME, Conf. Calcul. Phase Diagrams Thermochem. Alloy Phases*, Milwaukee, Wis, 17-18 Sept., 1979, Warrendale, Pa., 185-196 (1979) (Experimental, Phase Diagram, Phase Relations, 19)

[1979Gor] Gordon, B.A., Worrell, W., Nagarajan, V., "Thermodynamic Predictions of the Behavior of Fe-Cr-Al Alloys in Coal Gasifier Environments", *Oxid. Met.*, **13**(1), 13-23 (1979) (Calculation, Experimental, Interface Phenomena, Phase Diagram, Thermodynamics, 9)

[1979Kay] Kay, D.A.R., "Thermodynamic Data from Oxygen Concentration Cells at 1500-1600°C", *Rev. Int. Hautes Temp. Refract.*, **16**(1), 21-32 (1979) (Experimental, Thermodynamics, 43)

[1979Kub] Kubaschewski, O., Alcock, C.B., "Metallurgical Thermochemistry", 5th Edition, *Int. Ser. Mat Sci. Technol.*, Pergamon Press, Vol. **24**, 238-239 (1979) (Review, Theory)

[1979Nec] Nechaev, Yu.S., Edigarov, V.S., Pustov, Yu.A., "Investigation of Iron Solubility in Aluminium and in Materials of SAP Type by Mössbauer Spectroscopy" (in Russian), *Izv. Vyss. Uchebn. Zaved., Chern. Metall.*, **5**, 92-97 (1979) (Experimental, Phase Relations, 14)

[1979Rou] Rousset, A., Paris, J., Chassagneux, F., "Importance of Reactivity of the Finely Divided Solids for the Synthesis of New Phases" (in French), *Ann. Chim. Fr.*, **4**, 115-122 (1979) (Experimental, Phase Relations, Thermodynamics, 20)

[1980Aki] Akimov, A.G., Kazanskiy, L.P., "Oxidizing and Composition of the Surface of an Al-Fe Alloy" (in Russian), *Izv. Akad. Nauk SSSR, Otd. Khim. Nauk*, **10**, 2201-2205 (1980) (Experimental, Phase Diagram, Phase Relations, 12)

[1980Ban] Ban-Ya, S., Chiba, A., Hikosaka, A., "Thermodynamics of Fe_tO-M_xO_y (M_xO_y = CaO, SiO_2, TiO_2 and Al_2O_3) Binary Melts Saturated with Solid Iron", *Austral.-Jap. Extractive Metall. Symp.,* Sydney, Australia 16-18 July 1980, Australian Inst. Min. Metall., **23**, 457-467 (1980) (Experimental, Thermodynamics, 22)

[1980Gus] Gustafsson, S., Mellberg, P.O., "On the Free Energy Interaction between some Strong Deoxidizers, Especially Calcium, Aluminum and Oxygen in Liquid Iron", in *Scaninject II, Injection Metal.*, *Proc. Conf*., Lulea, Sweden, **20**(23), 1-19 (1980) (Thermodynamics, 7)

[1980Kli] Klissurski, D.G., Mitov, I.G., Petrov, K.P., "A Study of the Preparation of Solid Solutions in the System αFe_2O_3-Al_2O_3", *Thermochim. Acta*, **41**(2), 181-186 (1980), doi:10.1016/0040-6031(80)80063-3 (Crystal Structure, Experimental, Phase Diagram, 17)

[1980Mey] Meyers, C.E., Mason, T.O., Petuskey, W.T., Halloran, J.W., Bowen, H.K., "Phase Equilibria in the System Fe-Al-O", *J. Am. Ceram. Soc.*, **63**(11-12), 659-663 (1980), doi:10.1111/j.1151-2916.1980.tb09856.x (Experimental, Phase Diagram, #, *, 20)

[1981Pet] Petric, A., Jacob, K.T., Alcock, C.B., "Thermodynamic Properties of Fe_3O_4-$FeAl_2O_4$ Spinel Solid Solutions", *J. Am. Ceram. Soc.*, **64**(11), 632-639 (1981), doi:10.1111/j.1151-2916.1981.tb15860.x (Thermodynamics, Experimental, 28)

[1981She] Shevtsov, V.E., "Thermodynamics of Oxygen Solutions in the Fe-Al System", *Russ. Metall. (Engl. Transl.)*, (1), 52-57 (1981) (Phase Relations, Phase Diagram, Experimental, Thermodynamics, #, 16)

[1982Kub] Kubaschewski, O., "*Iron - Binary Phase Diagrams*", Springer Verlag, Berlin, Verlag Stahl Eisen, Düsseldorf, 5-9 and 79-82 (1982) (Phase Relations, Phase Diagram, Review, #, 32)

[1982Lia] Liang, W.W., "Prediction of Solubility of Oxides in Liquid Fe-Al-O, Co-Al-O, Ni-Al-O and Cu-Al-O Alloy", *Z. Metallkd.*, **73**(6), 369-375 (1982), doi:10.1515/ijmr-1982-730604 (Thermodynamics, Phase Relations, Phase Diagram, Theory, #, *, 31)

[1983Boj] Bojarski, Z., Isakow, Z., "Investigations of Al^{3+} and Ga^{2+} Solid Solutions in αFe_2O_3 Oxide" (in Polish), *Archiw. Nauki Mater.*, **4**(1), 3-20 (1983) (Experimental, #, 23)

[1983Elr] Elrefaie, F.A., Smeltzer, W.W., "Thermodynamics of the System Iron-Aluminium-Oxygen Between 1073 K and 1573 K", *Metall. Trans. B*, **14B**, 85-93 (1983), doi:10.1007/BF02654055 (Phase Relations, Phase Diagram, Experimental, Thermodynamics, #, 31)

[1983Yam] Yamauchi, S., Nakamura, A., Shimizu, T., Fueki, K., "Vacancy Diffusion in Magnetite-Hercynite Solid Solution", *J. Solid State Chem.*, **50**, 20-32 (1983) (Experimental, Theory, Thermodynamics, 21)

[1984Mac] Mackenzi, K.J.D., Brown, I.W.M., "The Mössbauer Spectrum and Structure of Iron(III) Aluminium Oxide, $FeAlO_3$", *J. Mater. Sci. Lett.*, **3**, 159-161 (1984) (Crystal Structure, Experimental, 8)

[1984Sch] Schuermann, E., Bannenberg, N., "Metal-Slag Equilibria in the System Iron-Aluminium-Oxygen as a Basis of Aluminium Deoxidation of Steel Melts" (in German), *Arch. Eisenhuettenwes.*, **55**(9), 409-414 (1984) (Phase Relations, Phase Diagram, Experimental, Thermodynamics, #, 27)

[1985Meh] Mehrotra, S.P., Chaklader, A.C.D., "Interfacial Phenomena between Molten Metals and Sapphire Substrate", *Metall. Trans. B*, **16B**, 567-575 (1985), doi:10.1007/BF02654855 (Experimental, 43)

[1985Tay] Taylor, D., "Thermal Expansion Data. VI. Complex Oxides, AB_2O_4, the Spinels", *British Ceram. Transact. J.*, **84**(4), 121-127 (1985) (Calculation, Crystal Structure, Review, 99)

[1985Wri] Wriedt, H.A., "The Al-O (Aluminium-Oxygen) System", *Bull. Alloy Phase Diagrams*, **6**(6), 548-553 (1985), doi:10.1007/BF02887157 (Phase Relations, Phase Diagram, Review, #, 46)

[1986Gho] Ghosh, A., Murthy, G.V.R., "An Assessment of Thermodynamic Parameters for Deoxidation of Molten Iron by Cr, V, Al, Zr and Ti", *Trans. Iron Steel Inst. Jpn.*, **26**(7), 629-637 (1986) (Assessment, Phase Diagram, Thermodynamics, 41)

[1988Ber] Berman, R.G., "Internally-Consistent Thermodynamic Data for Minerals in the System Na_2O-K_2O-CaO-MgO-FeO-Fe_2O_3-Al_2O_3-SiO_2-TiO_2-H_2O-CO_2", *J. Petrol.*, **29**, 445-552 (1988) (Review, Thermodynamics, 419)

[1988Was] Wasai, K., Mukai, K., "Thermodynamic Analysis of Fe-Al-O Liquid Alloy Equilibrated with α-Al_2O_3(s) by an Associated Solution Model", *J. Japan Inst. Metals*, **52**(11), 1088-1097 (1988) (Thermodynamics, 30)

[1989Rag1] Raghavan, V., "The Al-Fe-O System", in "*Phase Diagrams of Ternary Iron Alloys, Part 5*", Indian Inst. of Metals, Calcutta, **5**, 10-28 (1989) (Phase Relations, Phase Diagram, Review, #, 29)

[1989Rag2] Raghavan, V., "The Fe-O System", in "*Phase Diagrams of Ternary Iron Alloys, Part 5"*, Indian Inst. of Metals, Calcutta, **5**, 5-8 (1989) (Phase Diagram, Crystal Structure, Review, 3)

[1990Hol] Holland, T.J.B., Powell R., "An Enlarged and Updated Internally Consistent Thermodynamic Dataset with Uncertainties and Correlations - the System K_2O-Na_2O-CaO-MgO-MnO-FeO-Fe_2O_3-Al_2O_3-TiO_2-SiO_2-C-H_2-O_2", *J. Metamorphic Geol.*, **8**, 89-124 (1990) (Review, Thermodynamics, 267)

[1990Kuz] Kuznetsov, V.M., Kulikov, I.S., "The Solubility and Activity of Oxygen in Fe-Co-Ni-Cu Alloys Containing Zr, Hf, and Al", *Russ. Metall.*, (2), 19-22 (1990), translated from *Izv. Akad. Nauk SSSR, Met.*, **2**, 19-22 (1990) (Thermodynamics, Experimental, 9)

[1990Tsu] Tsuchida, T., Sugimoto, K., "Effect of Grinding of Mixtures of Goethite and Hydrated Alumina on the Formation of Fe_2O_3-Al_2O_3 Solid Solutions", *Thermochim. Acta*, **170**, 41-50 (1990) (Experimental, Phase Relations, 50)

[1991Nak] Nakashima, K., Takihira, K., Mori, K., Shinozaki, N., "Wettability of Al_2O_3 Substrate by Liquid Iron - Effects of Oxygen in Liquid Iron and Purity of Al_2O_3 Substrate" (in Japanese), *J. Jpn. Inst. Met.*, **55**(11), 1199-1206 (1991) (Experimental, Interface Phenomena, Phase Relations, 28)

[1991Skl] Sklad, P.S., McHargue, C.J., Romana, L., White, C.W., McCallum, J.C., "The Effect of Post-Implantation Annealing on the Microstructure of Al_2O_3 Implanted with Iron at 185°C", *Nucl. Instrum. Methods Phys. Res./B*, **B59-B60**(II), 1187-1194 (1991) (Morphology, Abstract, 7)

[1991Sun] Sundman, B., "An Assessment of the Fe-O System", *J. Phase Equilib.*, **12**(1), 127-140 (1991), doi:10.1007/BF02645709 (Phase Relations, Assessment, 53)

[1991Yao] Yao, T., Maki, J., Jinno, H., "Decomposition of Iron Spinel under Low Oxygen Partial Pressure" (in Japanese), *J. Ceram. Soc. Jpn.*, **99**(7), 639-641 (1991) (Crystal Structure, Experimental, 13)

[1992Hol] Holcomb, G.R., Pierre, G.R.St., "The Solubility of Alumina in Liquid Iron", *Metall. Trans. B*, **23B**, 789-790 (1992), doi:10.1007/BF02656457 (Thermodynamics, Experimental, 12)

[1992Kub] Kubaschewski, O., Schmid-Fetzer, R., "Aluminium–Iron–Oxygen", in *"Ternary Alloys"* Compr. Comp. Eval. Const. Data Phase Diagr., Petzow, G., Effenberg G. (Eds.), Weinheim; Basel (Switzerland); Cambridge; NY: VCH, **5**, 325-353 (1992), (Crystal Structure, Phase Diagram, Phase Relations, Assessment, *, 51)

[1992Sui] Suito, H., Inoue, R., Nagatani, A., "Mullite as an Electrochemical Probe for the Determination of Low Oxygen Activity in Liquid Iron", *Steel Res.*, **63**(10), 419-425 (1992), doi:10.1002/srin.199201735 (Experimental, Thermodynamics, 20)

[1992Tay] Taylor, J.R., Dinsdale, A.T., Hillert, M., Selleby, M., "A Critical Assessment of Thermodynamic and Phase Diagram Data for the Al-O System", *Calphad*, **16**(2), 173-179 (1992) (Calculation, Phase Diagram, Thermodynamics, 22)

[1992Tru] Trumble, K.P., "Thermodynamic Analysis of Aluminate Formation at Fe/Al_2O_3 and Cu/Al_2O_3 Interfaces", *Acta Metall. Mat., Suppl.*, **40**, S105-S110 (1992) (Thermodynamics, 30)

[1993Eri] Eriksson, G., Wu, P., Pelton, A.D., "Critical Evaluation and Optimization of the Thermodynamic Properties and Phase Diagrams of the MgO-Al_2O_3, MnO-Al_2O_3, FeO-Al_2O_3 and K_2O-Al_2O_3 Systems", *Calphad*, **17**(2), 189-205 (1993), doi:10.1016/0364-5916(93)90019-8 (Phase Diagram, Review, 74)

[1993Kat] Kattner, U.R., Burton, B.P., "Al-Fe (Aluminum-Iron)", *Phase Diagrams of Binary Iron Alloys*, Okamoto, H. (Ed.), Mater. Park OH: ASM Int., 12-28 (1993) (Crystal Structure, Electrical Properties, Magnetic Properties, Mössbauer, Phase Diagram, Review, Thermodynamics, *, 99)

[1993Kub] Kubaschewski, O., Alcock, C.B., Spencer, P.J., "*Materials Thermochemistry*", Pergamon Press, Oxford (1993)

[1993Sax] Saxena, S.K., Chatterjee, N., Fei, Y., Shen, G., "*Thermodynamic Data on Oxides and Silicates*", Springer Verlag (1993)

[1993Tyu] Tyurin, A.G., "Thermodynamics of Molecular and Ionic Solutions", *Russ. Metall. (Engl. Transl.)*, (2), 39-47 (1993), translated from *Izv. RAN, Met.*, (2), 48-56 (1993) (Theory, Thermodynamics, 35)

[1994Bur] Burkhardt, U., Grin, J., Ellner, M., Peters, K., "Structure Refinement of the Iron-Aluminium Phase with the Approximate Composition Fe_2Al_5", *Acta Crystallogr., Sect. B.*, **B50**, 313-316 (1994), doi:10.1107/S0108768193013989 (Crystal Structure, Experimental, *, 9)

[1995Bar] Barin, I., "Thermochemical Data for Pure Substances", Wiley-VCH, New-York (1995) (Thermodynamics, Review)

[1995Bou] Bouchard, D., Bale, C.W., "Thermochemical Properties of Iron-Rich Liquid Solutions Containing Oxygen and Aluminium", *J. Phase Equilib.*, **16**(1), 16-23 (1995), doi:10.1007/BF02646244 (Thermodynamics, 29)

[1995Dim] Dimitrov, S., Weyl, A., Janke, D., "Control of the Aluminum-Oxygen Reaction in Pure Melts", *Steel Res.*, **66**(1), 3-7 (1995) (Experimental, Phase Relations, Thermodynamics, 29)

[1995Esc] Escribano, V.S., Amores, J.M.G., Finocchio, E., Daturi, M., Busca, G., "Characterization of α-$(Fe,Al)_2O_3$ Solid-Solution Powders', *J. Mater. Chem.*, **5**(11), 1943-1951 (1995) (Crystal Structure, Experimental, 44)

[1995Jow] Jowsa, J., "Phase Equilibrium of Fe-O-I Systems (I = Ca, Al) Used for Steelmaking", *Hutnik-Wiadomosci Hutnicze*, **8**, 301-304 (1995) (Phase Diagram, Thermodynamics, Calculation, 13)

[1996Bou] Bouree, F., Baudour, J.L., Elbadraoui, E., Musso, J., Laurent, C., Rousset, A., "Crystal and Magnetic Structure of Piezoelectric, Ferrimagnetic and Magnetoelectric Aluminium Iron Oxide $FeAlO_3$ from Neutron Powder Diffraction', *Acta Crystallogr., Sect. B: Struct. Crystallogr. Crys. Chem.*, **B52**(2), 217-222 (1996), doi:10.1107/S0108768195010330 (Crystal Structure, Experimental, 10)

[1996Lee] Lee, H.Y., Rhee, Y.W., Kang, S.J.L., "Discontinuous Dissolution and Grain-Boundary Migration in Al_2O_3-Fe_2O_3 by Oxygen Partial Pressure Change", *J. Am. Ceram. Soc.*, **79**(6), 1659-1663 (1996) (Experimental, Morphology, Phase Diagram, Phase Relations, 24)

[1997Ito] Itoh, H., Hino, M., Banya, S., "Assessment of Al Deoxidation Equilibrium in Liquid Iron", *J. Iron Steel Inst. Jpn.*, **83**(12), 773-778 (1997) (Experimental, Thermodynamics, 17)

[1997Got] Gottschalk, M., "Internally Consistent Thermodynamic Data for Rock-Forming Minerals in the System SiO_2-TiO_2-Al_2O_3-Fe_2O_3-CaO-MgO-FeO-K_2O-Na_2O-H_2O-CO_2", *Eur. J. Mineral.*, **9**, 175-223 (Review, Thermodynamics, Calculation, 246)

[1997Li] Li, G.Q., Suito, H., "Electrochemical Measurement of Critical Supersaturation in Fe-O-M (M = Al, Si, and Zr) and Fe-O-Al-M (M = C, Mn, Cr, Si, and Ti) Melts by Solid Electrolyte Galvanic Cell", *ISIJ Int.*, **37**(8), 762-769 (1997), doi:10.2355/isijinternational.37.762 (Experimental, Phase Relations, Electrochemistry, 26)

[1997Sub] Subramanian, R., McKamey, C.G., Buck, L.R., Schneibel, J.H., "Synthesis of Iron Aluminide-Al_2O_3 Composites by *In-situ* Displacement Reactions", *Mater. Sci. Eng. A*, **239-240**, 640-646 (1997) (Experimental, Mechanical Properties, Morphology, Phase Diagram, Phase Relations, 23)

[1998Cos] Da Costa, G.M., De Grave, E., Vandenberghe, R.E., "Mössbauer Studies of Magnetite and Al-Substituted Maghemites", *Hyperfine Interact.*, **117**, 207-243 (1998) (Crystal Structure, Experimental, 77)

[1998Har] Harrison, R.J., Redfern, S.A.T., O'Neill, H.S.C., "The Temperature Dependence of the Cation Distribution in Synthetic Hercynite ($FeAl_2O_4$) from *in-situ* Neutron Structure Refinements", *Am. Mineral.*, **83**, 1092-1099 (1998), doi:10.2138/am-1998-9-1018 (Experimental, Crystal Structure, Theory, 35)

[1998Seo] Seo, J.-D., Kim, S.-H., Lee, K.-R., "Thermodynamic Assessment of the Al Deoxidation Reaction in Liquid Iron", *Steel Res.*, **69**(2), 49-53 (1998), doi:10.1002/srin.199801342 (Experimental, Thermodynamics, 16)

[1999Fuj] Fujiwara, H., Hattori, A., Ichise, E., "Equilibrium Between Aluminum and Oxygen in Fe-36%Ni Alloy and Liquid Iron at 1973K" (in Japanese), *J. Iron Steel Inst. Jpn.*, **85**(3), 201-207 (1999) (Experimental, Thermodynamics, 14)

[1999Ma] Ma, Z., Janke, D., "Oxygen and Nitrogen Reactions in Fe-X and Fe-Cr-Ni-X Melts", *Steel Res.*, **70**(10), 395-402 (1999), doi:10.1002/SRIN.199905658 (Calculation, Thermodynamics, 69)

[1999Mei] Mei, J., Halldearn, R.D., Xiao, P., "Mechanisms of the Aluminium-Iron Oxide Thermite Reaction", *Scr. Mater.*, **41**(5), 541-548 (1999) (Crystal Structure, Experimental, Morphology, Phase Diagram, 8)

[1999Was1] Wasai, K., Mukai, K., "Thermodynamics of Nucleation and Supersaturation for the Aluminum-Deoxidation Reaction in Liquid Iron", *Metall. Mater. Trans. B*, **30**(6), 1065-1074 (1999) (Calculation, Thermodynamics, 17)

[1999Was2] Wasai, K., Mukai, K., Fuchiwaki, H., Yoshida, A., "Determination of Aluminum and Oxygen Contents in Liquid Iron in Equilibrium With α-Alumina and Hercynite", *ISIJ Int.*, **39**(8), 760-766 (1999) (Experimental, Morphology, Phase Relations, 17)

[1999Yok] Yokokawa, H., "Generalized Chemical Potential Diagram and Its Applications to Chemical Reactions at Interfaces between Dissimilar Materials", *J. Phase Equilib.*, **20**(3), 258-287 (1999), doi:10.1361/105497199770335794 (Phase Relations, Review, 93)

[2000Ban] Banovic, S.W., Dupont, J.N., Marder, A.R., "The Use of Ternary Phase Diagrams in the Study of High Temperature Corrosion Products Formed on Fe-5wt% Al Alloys in Reducing and Oxidizing Environments", *Acta Mater.*, **48**(11), 2815-2822 (2000) (Experimental, Interface Phenomena, Morphology, Phase Diagram, Phase Relations, 34)

[2000Bjo] Bjoerkvall, J., Sichen, D., Seetharaman, S., "Thermodynamic Description of Al_2O_3-CaO-MnO and Al_2O_3-FeO-MnO Melts - A Model Approach", *Calphad*, **24**(3), 353-376 (2000), doi:10.1016/S0364-5916(01)00010-4 (Assessment, Calculation, Phase Relations, Thermodynamics, 18)

[2000Jan] Janke, D., Ma, Z.T., Valentin, P., Heinen, A., "Improvement of Castability and Quality of Continuously Cast Steel", *ISIJ Int.*, **40**(1), 31-39 (2000) (Theory, Thermodynamics, 46)

[2001Ike] Ikeda, O., Ohnuma, I., Kainuma, R., Ishida, K., "Phase Equilibria and Stability of Ordered *BCC* Phases in the Fe-rich Portion of the Fe-Al System", *Intermetallics*, **9**, 755-761 (2001) (Experimental, Mechanical Properties, Phase Relations, 18)

[2001Jha] Jha, R., Haworth, C.W., Argent, B.B., "The Formation of Diffusion Coating on Some Low-Alloy Steels and Their High Temperature Oxidation Behaviour: P_2 Oxidation Studies", *Calphad*, **25**(4), 667-689 (2001) (Calculation, Phase Relations, 35)

[2001Lad] Ladavos, A.K., Bakas, T.V., "The Al_2O_3-Fe_2O_3 Mixed Oxidic System, I. Preparation and Characterization", *React. Kinet. Catal. Lett.*, **73**(2), 223-228 (2001) (Crystal Structure, Experimental, Phase Relations, 10)

[2001Mas] Masahashi, N., Watanabe, S., Hanada, Sh., "Microstructure and Oxidation Behaviour of Low Pressure Plasma Sprayed Iron Aluminides", *ISIJ Int.*, **41**(9), 1010-1017 (2001) (Crystal Structure, Experimental, Mechanical Properties, 16)

[2001Sas] Sasai, K., Mizukami, Y., "Mechanism of Alumina Adhesion to Continuous Caster Nozzle with Reoxidation of Molten Steel", *ISIJ Int.*, **41**(11), 1331-1339 (2001) (Experimental, Interface Phenomena, Morphology, 22)

[2001Sur] Suryanarayana, C., "Mechanical Alloying and Milling", *Prog. Mater. Sci.*, **46**(1-2), 1-184 (2001) (Crystal Structure, Experimental, Kinetics, Phase Relations, Review, Thermodynamics, 932)

[2002Bot] Botta, P.M., Bercoff, P.G., Aglietti, E.F., Bertorello, H.R., Lopez, J.M.P., "Magnetic and Structural Study of Mechanochemical Reactions in the Al-Fe_3O_4 System", *J. Mater. Sci.*, **37**(12), 2563-2568 (2002) (Crystal Structure, Experimental, Magnetic Properties, Morphology, Phase Relations, 25)

[2002Dav] Davies, R.H., Dinsdale, A.T., Gisby, J.A., Robinson, J.A.J., Martin, S.M., "MTDATA - Thermodynamic and Phase Equilibrium Software from the National Physical Laboratory", *Calphad*, **26**(2), 229-271 (2002) (Calculation, Phase Relations, Thermodynamics, 29)

[2002Gos] Da Gosta, G.M., Van San, E., De Grave, E., Vanderberghe, R.E., Barron, V., Datas, L., "Al Hematites Prepared by Homogeneous Precipitation of Oxinates: Material Characterization and Determination of the Morin Transition", *Phys. Chem. Miner.*, **29**, 122-131 (2002) (Crystal Structure, Experimental, Magnetic Properties, 24)

[2002Gra] Granovskii, A., Sato, H., Aoki, Y., Yurasov, A., "Tunneling Thermopower in Magnetic Granular Alloys", *Phys. Solid State*, **44**(11), 2095-2097 (2002) (Calculation, Magnetic Properties, Theory, 10)

[2002Maj] Majzlan, J., Navrotsky, A., Evans, B.J., "Thermodynamics and Crystal Chemistry of the Hematite-Corundum Solid Solution and the $FeAlO_3$ Phase", *Phys. Chem. Miner.*, **29**(8), 515-526 (2002), doi:10.1007/s00269-002-0261-7 (Thermodynamics, Crystal Structure, Experimental, 43)

[2002Tak] Takacs, L., "Self-Sustaining Reactions Induced by Ball Milling", *Prog. Mater. Sci.*, **47**, 355-414 (2002) (Experimental, Kinetics, Mechanical Properties, Review, Theory, Thermodynamics, 192)

[2002Was] Wasai, K., Mukai, K., "Thermodynamic Analysis on Metastable Alumina Formation in Aluminum Deoxidized Iron Based on Ostwalds Step Rule and Classical Homogeneous Nucleation Theories", *ISIJ Int.*, **42**(5), 467-473 (2002) (Calculation, Thermodynamics, 20)

[2003Bot] Botta, P.M., Mercader, R.C., Aglietti, E.F., Lopez, J.M.P., "Synthesis of Fe-$FeAl_2O_4$-Al_2O_3 by High-Energy Ball Milling of Al-Fe_3O_4 Mixtures", *Scr. Mater.*, **48**(8), 1093-1098 (2003) (Crystal Structure, Experimental, Phase Relations, 16)

[2003Kap] Kapilashrami, E., Jakobsson, A., Lahiri, A.K., Seetharaman, S., "Studies of the Wetting Characteristics of Liquid Iron on Dense Alumina by X-Ray Sessile Drop Technique", *Metall. Mater. Trans. B*, **34B**(2), 193-199 (2003) (Phase Diagram, Thermodynamics, 18)

[2003Kle] Klemme, S., van Miltenburg, J.C., "Thermodynamic Properties of Hercynite ($FeAl_2O_4$) Based on Adiabatic Calorimetry at Low Temperatures", *Am. Mineral.*, **88**, 68-72 (2003), doi:10.2138/am-2003-0108 (Experimental, Thermodynamics, 42)

[2003Lan] Lang, F., Yu, Zh., Gedevanishvili, Sh., Deevi, S.C., Narita, T., "Effect of Pre-Oxidation on the Corrosion Behaviour of Fe-40Al Sheet in a N_2-11.2O_2-7.5CO_2-500 ppm SO_2 Atmosphere at 1273 K", *Intermetallics*, **11**(2), 129-134 (2003) (Experimental, Interface Phenomena, 24)

[2003Mun] Munoz-Morris, M.A., Garcia Oca, C., Morris, D.G., "Microstructure and Room Temperature Strength of Fe-40Al Containing Nanocrystalline Oxide Particles", *Acta Mater.*, **51**(17), 5187-5197 (2003) (Experimental, Mechanical Properties, Morphology, 32)

[2003Xue] Xue, D.S., Huang, Y.L., Ma, Y., Zhou, P.H., Niu, Z.P., Li, F.S., Job, R., Fahrner, W.R., "Magnetic Properties of Pure Fe-Al_2O_3 Nanocomposites", *J. Mater. Sci. Lett.*, **22**(24), 1817-1820 (2003) (Experimental, Magnetic Properties, Morphology, 17)

[2004Cot] Cotica, L.F., Zanatta, S.C., de Medeiros, S.N., dos Santos, I.A., Paesano, A., da Cunha, J.B.M., "Mechanical Milling of the $(\alpha\text{-}Fe_2O_3)_{(x)}(\alpha\text{-}Al_2O_3)_{(1-x)}$ System: an X-ray Diffraction and Mössbauer Spectral Study", *Solid State Ionics*, **171**(3-4), 283-288 (2004), doi:10.1016/j.ssi.2004.04.018 (Crystal Structure, Electronic Structure, Experimental, 27)

[2004Fab] Fabrichnaya, O.B., Saxena, S.K., Richet, P., Westrum, E.F., "*Thermodynamic Data, Models and Phase Diagrams in Multicomponent Oxide Systems*", Springer-Verlag, Berlin, Heidelberg (2004) (Review, Thermodynamics)

[2004Fre] Fredriksson. P., Seetharaman, S., "Thermodynamics Activities of FeO in some Binary FeO-Containing Slags", *Steel Res.*, **75**, 240-246 (2004), doi:10.1002/srin.200405951 (Calculation, Experimental, Thermodynamics, 23)

[2004Vil] Villafuerte-Castrejon, M.E., Castillo-Pereyra, E., Tartaj, J., Fuentes, L., Bueno-Baques, D., Gonzalez, G., Matutes-Aquino, J.A., "Synthesis and AC Magnetic Susceptibility Measurements of $Fe_{2-x}Al_xO_3$ Compounds", *J. Magn. Magn. Mater.*, **272-276**(2), 837-839 (2004) (Crystal Structure, Experimental, Magnetic Properties, Physical Properties, 7)

[2005Fee] Feenstra, A., Saemann, S., Wunder, B., "An Experimental Study of Fe-Al Solubility in the System Corundum-Hematite up to 40 kbar and 1300°C", *J. Petrology*, **46**(9), 1881-1892 (2005), doi:10.1093/petrology/egi038 (Crystal Structure, Phase Relations, Thermodynamics, 36)

[2005Liu] Liu, M., Li, H.B., Xiao, L., Yu, W.X., Lu, Y., Zhao, Z.D., "XRD and Mössbauer Spectroscopy Investigation of Fe_2O_3-Al_2O_3 Nano-Composite", *J. Magn. Magn. Mater.*, **294**(3), 294-297 (2005) (Crystal Structure, Experimental, 8)

[2007Kub] Kubaschewski, O., Schmid-Fetzer, R., Rokhlin, L., Cornish, L., Fabrichnaya, O., "Al-Fe-O Ternary Phase Diagram Evaluation", in *MSI Eureka*, Effenberg, G. (Ed.), MSI, Materials Science International Services GmbH, Stuttgart (2007), Document ID: 10.11481.2.2 (Crystal Structure, Phase Diagram, Phase Relations, Assessment, *, 154)

[2007Ste] Stein, F., Palm, M., "Re-Determination of Transition Temperatures in the Fe-Al System by Differential Thermal Analysis", *Int. J. Mater. Res.* (*Z. Metallkd.*), **98**(7), 580-588 (2007), doi:10.1016/j.calphad.2008.01.002 (Experimental, Phase Diagram, Phase Relations, *, 59)

[2008Gil] Gille, P., Bauer, B., "Single Crystal Growth of $Al_{13}Co_4$ and $Al_{13}Fe_4$ from Al-Rich Solutions by the Czochralski Method", *Cryst. Res. Technol.*, **43**(11), 1161-1167 (2008), doi:10.1002/crat.200800340 (Crystal Structure, Experimental, Morphology, Phase Relations, Theory, 17)

[2010Chu] Chumak, I., Richter, K.W., Ehrenberg, H., "Redetermination of Iron Dialuminide, $FeAl_2$", *Acta Crystallogr. C*, **66**, i87-i88 (2010), doi:10.1107/S0108270110033202 (Experimental, Crystal Structure, 10)

[2010Ste] Stein, F., Vogel, S.C., Eumann, M., Palm, M., "Determination of the Crystal Structure of the ε Phase in the Fe-Al System by High-Temperature Neutron Diffraction", *Intermetallics*, **18**(1), 150-156 (2010), doi:10.1016/j.intermet.2009.07.006 (Crystal Structure, Experimental, Phase Relations, 40)

[2009Rha] Rhamdhani, M.A., Hidayat, T., Hayes, P.C., Jak, E., "Subsolidus Phase Equilibria of Fe-Ni-X-O (X = Mg, Al) Systems in Air", *Metall. Mater. Trans. B*, **40**(1), 25-38 (2009), doi:10.1007/s11663-008-921 (Calculation, Experimental, Phase Diagram, Thermodynamics, 38)

[2010Pop] Popcevic, P., Smontara, A., Ivkov, J., Wencka, M., Komelj, M., Jeglic, P., Vrtnik, S., Bobnar, M., Jaglicic, Z., Bauer, B., Gille, P., Borrmann, H., Burkhardt, U., Grin, Yu., Dolinsek, J., "Anisotropic Physical Properties of the $Al_{13}Fe_4$ Complex Intermetallic and its Ternary Derivative $Al_{13}(Fe,Ni)_4$", *Phys. Rev. B: Condens. Matter*, **81**(18), 184203 (2010), doi:10.1103/PhysRevB.81.184203 (Crystal Structure, Electrical Properties, Experimental, Magnetic Properties, Physical Properties, Thermodynamics, Transport Phenomena, 42)

[2011Lyk] Lykasov, A.A., Kimyashev, A.A., "Activities of the Components in a Spinel Solid Solution of the Fe-Al-O System", *Russ. J. Phys. Chem. A*, **85**(9), 1495-1498 (2011), doi:10.1134/S0036024411090135, Translated from *Zhurnal Fizicheskoi Khimii*, **85**(9), 1612-1614 (2011) (Electrochemistry, Experimental, Thermodynamics, 8)

[2015Lin] Lindwall, G., Liu, X.L., Ross, A., Fang, H., Zhou, B.-C., Liu, Z.-K., "Thermodynamic Modeling of the Aluminum-Iron-Oxygen System", *Calphad*, **51**, 178-192 (2015), doi:10.1016/j.calphad.2015.09.004 (Assessment, Phase Diagram, Review, Thermodynamics, 80)

[2016Li] Li, X., Scherf, A., Heilmaier, M., Stein, F., "The Al-Rich Part of the Fe-Al Phase Diagram", *J. Phase Equilib. Diffus.*, **37**, 162-173 (2016), doi:10.1007/s11669-015-0446-7 (Crystal Structure, Experimental, Phase Diagram, Phase Relations, 38)

[2016Shi] Shishin, D., Prostakova, V., Jak, E., Decterov, S.A., "Critical Assessment and Thermodynamic Modeling of the Al-Fe-O System", *Metall. Mater. Trans. B*, **47**(1), 397-424 (2016), doi:10.1007/s11663-015-0493-9 (Assessment, Calculation, Phase Diagram, Thermodynamics, 108)

[2016Dre] Dreval, L., Zienert, T., Fabrichnaya, O., "Calculated Phase Diagrams and Thermodynamic Properties of the Al_2O_3-Fe_2O_3-FeO System", *J. Alloys Compd.*, **657**, 192-214 (2016), doi:10.1016/j.jallcom.2015.10.017 (Assessment, Calculation, Phase Diagram, Thermodynamics, 73)

[2018Dre] Dreval, L., Zienert, T., Fabrichnaya, O., "Corrigendum to 'Calculated Phase Diagrams and Thermodynamic Properties of the Al_2O_3-Fe_2O_3-FeO system' (*J. Alloys Compd.,* **657** (2016) 192-214)", *J. Alloys Compd.*, **734**, 346 (2018), doi:10.1016/j.jallcom.2017.10.240 (Calculation, Phase Diagram, Phase Relations, Thermodynamics, 1)

[2020Agc] Agca, C., Lindwall, G., McMurray, J.W., Neuefeind, J.C., Liu, Z.-K., Navrotsky, A., "Experimental and Computational Studies of Melting of the Spinel Phase in the Fe-Al-O Ternary System", *Calphad*, **70**, 101798 (2020), doi:10.1016/j.calphad.2020.101798 (Calculation, Experimental, Phase Relations, Thermodynamics, 35)

[2021Ham] Hamada, T., Higashi, M., Niitsu, K., Inui, H., "Phase Equilibria among η-Fe_2Al_5 and its Higher-Ordered Phases", *Sci. Technol. Adv. Mater.*, (2021), doi:10.1080/14686996.2021.1915691 (Experimental, Crystal Structure, Phase Relations, Phase Diagram, *, 31)

[2022Ste] Stein, F., "Al-Fe Binary Phase Diagram Evaluation", in *MSI Eureka*, Watson, A. (Ed.), MSI, Materials Science International Services GmbH, Stuttgart (2022), Document ID: 20.10236.2.7 (2022), doi:10.7121/msi-eureka-20.10236.2.7 (Crystal Structure, Phase Diagram, Assessment, 311)

Table 1: Investigations of the Al-Fe-O Phase Relations, Structures and Thermodynamics

Reference	Method/Experimental Technique	Temperature/Composition/Phase Range Studied
[1995Bou]	Modeling, thermodynamic calculation	1600-1866°C/Alumina solubility in liquid Fe
[1995Dim]	EMF technique, thermodynamic calculation	1600°C/up to 1 mass% Al, 10^{-5} - 0.02 mass% O
[1995Esc]	X-ray diffraction, Fourie-transform infrared and diffuse reflectance ultraviolet-visible spectroscopy	400-900°C/Fe_2O_3-Al_2O_3
[1995Jow]	Thermodynamic calculation	~1600°C/10^{-4}- ~2 mass% Al, $1.8\cdot10^{-4}$ - 0.2 mass% O
[1996Bou]	Neutron diffraction, high resolution diffractometer	Room temperature and 30 K/$FeAlO_3$
[1996Lee]	X-ray diffraction, EDS	Annealed at 1500°C/Al_2O_3-Fe_2O_3
[1997Ito]	Thermodynamic calculation	1500-1900°C/10^{-4} - 10^2 mass% Al, 10^{-5} - $2\cdot10^2$ mass% O
[1997Li]	Electrochemical measurements, EMF technique	1600°C/$2.5\cdot10^{-4}$ - 0.3 mass% Al, $4\cdot10^{-4}$ - $7\cdot10^{-2}$ mass% O
[1998Cos]	Mössbauer spectroscopy, XRD	8-475 K/$(Fe_{1-y}Al_y)_2O_3$ with y = 0-0.66

Reference	Method/Experimental Technique	Temperature/Composition/Phase Range Studied
[1998Har]	Neutron powder diffraction	25-1150°C/ $FeAl_2O_4(\sigma)$
[1998Seo]	Thermodynamic assessment, chemical analysis for determination of equilibrium composition	1600°C/$2\cdot10^{-4}$ - 0.99 mass% Al, $1.1\cdot10^{-3}$ - 0.011 mass% O
[1999Ma]	Thermodynamic calculation	1600°C/10^{-4} - 0.05 mass% Al
[1999Mei]	Chemical reaction between powders, DTA, SEM, XRD	20-1060°C/Al-Fe_2Al_3
[1999Was1]	Computer simulation, thermodynamic calculation	1600°C/0.01 - 0.1 mass% Al, 0.005 - 0.025 mass% O
[1999Was2]	Alloys prepared by heating mixtures of components, selective chemical analysis, XRD	1600°C/Fe-$FeAl_2O_4$
[1999Yok]	Phase diagram calculation	1300°C 3D potential diagram
[2000Ban]	EPMA, EDS	700°C, Fe-5 mass% Al oxidizing environment
[2000Bjo]	Thermodynamic calculation	1400°C, FeO-Al_2O_3 system, $x(Al_2O_3)$ = 0-0.1
[2001Jha]	Phase diagram calculation MTDATA, NPL database	1000°C, Al-Fe 0-100 mass% $p(O_2) = 10^{-15}$ - 10^5 Pa
[2001Lad]	XRD, Mössbauer spectroscopy	1150°C synthesis, 25°C measurements
[2001Mas]	XRD, SEM-EDX	700-1000° Fe-40 at.% Al in air
[2002Bot]	Mechanical milling, XRD, magnetic properties, DTA, SEM	room temperature/ Al-Al_2O_3-$FeAl_2O_4$-Fe_3O_4-Fe
[2002Gos]	XRD, thermal analysis, FTIR spectroscopy, optical reflection analysis, TEM, Mössbauer spectra	80, 298 K Fe_2O_3-Al_2O_3 system up to 10% Al_2O_3
[2002Dav]	Phase diagram calculation MTDATA, NPL database	900-2100°C Fe_2O_3-Al_2O_3 system in air
[2002Maj]	HT oxide-melt drop calorimetry, DS calorimetry, Rietveld refinement of XRD, Mössbauer spectroscopy, calculation	200-1550 K, $FeAlO_3$, C_p; 25, 602°C Fe_2O_3-Al_2O_3 system, $\Delta H°_f$,oxides; 25°C, $FeAlO_3$, $S°$
[2002Was]	Modelling of process, thermodynamic calculation	1600°C/Fe-Al_2O_3
[2003Bot]	Mechanical milling, XRD, Mössbauer spectroscopy, DTA	room temperature/ x(Al) + y(Fe_3O_4) at x:y = 2.67:1
[2003Kap]	Contact angle measurement by X-ray sessile-drop method	1550-1600°C Fe-Al_2O_3 system $p(O_2$ in Ar) ≤10 - 14 Pa 1550°C $p(O_2)$=$9.9\cdot10^{-4}$, $3\cdot10^{-3}$ Pa (CO/CO_2+Ar)
[2003Kle]	Adiabatic calorimetry	3-400 K; $FeAl_2O_4(\sigma)$
[2004Cot]	Mechanical milling, XRD, Mössbauer spectroscopy	room temperature/$(\alpha Fe_2O_3)_x(\alpha Al_2O_3)_{1-x}$ with $0.10 \le x \le 0.50$
[2004Fre]	Slag-metal equilibrium technique, chemical analysis, thermodynamic modelling	1400 - 1600°C/FeO-Al_2O_3
[2004Vil]	XRD, density measurement by picknometry	25°C, $Fe_{2-x}Al_xO_3$, $0.9 \le x \le 1.08$
[2005Fee]	Synthesis of materials by sintering powders, EPMA	800 - 1300°C/ Al_2O_3-Fe_2O_3
[2005Liu]	Preparation of Fe_2O_3-Al_2O_3 nanocomposites by sol-gel means, XRD, Mössbauer spectroscopy	500 - 1100°C/ Fe_2O_3-Al_2O_3
[2009Rha]	Equilibration and quenching technique, optical microscopy, SEM-EDS, EPMA	1200, 1300, 400°C, p_{O2} = 0.21 atm/ Fe_2O_3-Al_2O_3

Reference	Method/Experimental Technique	Temperature/Composition/Phase Range Studied
[2011Lyk]	Emf measurements, galvanic cell with solid electrolyte	700, 870, 900, 1000°C/ Activity of Fe_3O_4 and $FeAl_2O_4$
[2015Lin]	Thermodynamic assessment, Calphad method	Oxide FeO-Fe_2O_3-Al_2O_3 part of the system
[2016Shi]	Thermodynamic assessment, Calphad method	Oxide FeO-Fe_2O_3-Al_2O_3 part of the system including the phases of the Al-Fe system
[2016Dre], [2018Dre]	Thermodynamic assessment, Calphad method	Oxide FeO-Fe_2O_3-Al_2O_3 part of the system
[2020Agc]	XRD, cooling trace experiments, DTA	Reducing atmosphere/ liquidus and solidus temperatures, $Fe_{3-x}Al_xO_4$

Table 2: Crystallographic Data of Solid Phases

Phase/ Temperature Range (°C)	Pearson Symbol/ Space Group/ Prototype	Lattice Parameters (pm)	Comments/References
(αAl) < 660.452	*cF*4 $Fm\bar{3}m$ Cu	*a* = 404.96	pure Al at 25°C [Mas2]
(αδFe) αFe ≤ 912	*cI*2 $Im\bar{3}m$ W	*a* = 286.65	Strukturbericht designation: *A*2 at 25°C [Mas2]
δFe 1538 - 1394		*a* = 293.15	at 1480°C [Mas2]
(γFe) 1394 - 912	*cF*4 $Fm\bar{3}m$ Cu	*a* = 364.67	at 915°C [V-C2, Mas2]
αAl_2O_3 < 2054	*hR*30 $R\bar{3}c$ Al_2O_3	*a* = 475.4 *c* = 1299	[V-C], corundum, congruent melting 2054°C [Mas2]
γAl_2O_3	*cF*56 $Fd\bar{3}m$ $MgAl_2O_4$	*a* = 794.7	[V-C2] metastable
$Fe_{1-x}O$ < 912	*cF8* $Fm\bar{3}m$ NaCl	*a* = 431.0 *a* = 429.3	*x* = 0.05, *x* = 0.12 [V-C2] wüstite, 51.15 to 54.6 at.% O
Fe_2O_3	*hR*30 $R\bar{3}c$ Al_2O_3	*a* = 503.42 *c* = 1374.83	[V-C], hematite, peritectoid formation at 1457°C, 1.013 bar p_{O2}
Fe_3Al < 545	*cF*16 $Fm\bar{3}m$ BiF_3		sometimes named α_1 phase Strukturbericht designation: $D0_3$ ~24 to ~34 at.% Al at 400°C [1993Kat]
		a = 579.3	at 23.1 at.% Al, water-quenched from 250°C [1958Tay]
		a = 578.86	at 35.0 at.% Al, water-quenched from 250°C [1958Tay]
FeAl < 1318	*cP*2 $Pm\bar{3}m$ CsCl		sometimes named α_2 phase Strukturbericht designation: *B*2 23.5 to ~53 at.% Al [2007Ste]
		a = 289.76 to 290.90	at 36.2 to 50.0 at.% Al, water-quenched from 250°C [1958Tay]

Phase/ Temperature Range (°C)	Pearson Symbol/ Space Group/ Prototype	Lattice Parameters (pm)	Comments/References
Fe_5Al_8 1231 - 1095	*cI*52 $I\bar{4}3m$ Cu_5Zn_8		sometimes named ε phase Strukturbericht designation: $D8_2$ 56.0 to 64.5 at.% Al [2016Li] at 1120°C and 59.4 at.% Al [2010Ste]
		a = 897.57±0.02	
$FeAl_2$ < 1146	*aP*19 $P\bar{1}$ $FeAl_2$		sometimes named ζ phase 64.9 to 66.7 at.% Al at 1000°C [2016Li] at 66.4 at.% Al [2010Chu]
		a = 487.45 b = 645.45 c = 873.61 α = 87.930° β = 74.396° γ = 83.062°	
Fe_2Al_5 1159 - ~331	*oC*24 *Cmcm* Fe_2Al_5		sometimes named η phase 70.0 to 72.5 at.% Al at 1000°C [2016Li, 2021Ham] at 71.5 at.% Al [1994Bur]
		a = 765.59 ± 0.08 b = 641.54 ± 0.06 c = 421.84 ± 0.04	
Fe_4Al_{13} < 1150	*mC*102 *C*2/*m* Fe_4Al_{13}		referred to as $FeAl_3$ in old literature before ~1995 sometimes named θ phase 74.6 to ~76.8 at.% Al at 1000°C [2016Li1]
		a = 1548.8±0.1 b = 808.66±0.05 c = 1247.69±0.08 β =(107.669±0.004)°	single crystal grown by Czochralski technique [2008Gil, 2010Pop]
$Fe_{3-x}Al_xO_4$	*cF*56 $Fd\bar{3}m$		0 ≤ x ≤ 2 above 860°C spinel
Fe_3O_4 < 1597	$MgAl_2O_4$	a = 839.6	at 25°C, x = 0, magnetite, 57.14 to 58.3 at.% O
$FeAl_2O_4$ < 1800		a = 815	at x = 2, hercynite, [1962Tur]
*$FeAlO_3$ 1410 - 1318	*oP*40 *Pna*2$_1$ $FeGaO_3$	a = 856.61 b = 924.91 c = 498.92	[1996Bou, 2004Vil] Homogeneity range is narrow and depends on partial pressure of oxygen

Table 3: Invariant Equilibria

Reaction	T (°C)	Type	Phase	Composition (at.%)		
				Al	Fe	O
L' ⇌ (αδFe) + Al_2O_3	1537.6	e_5	L'	$1.03 \cdot 10^{-2}$	99.98	$1.12 \cdot 10^{-3}$
L' + Al_2O_3 ⇌ (αδFe) + σ	1535.5	U_1	L'	$8.48 \cdot 10^{-6}$	99.87	0.1255
L' + σ ⇌ L'' + (αδFe)	1528.5	U_2	L'	$8.05 \cdot 10^{-7}$	99.52	0.48

Table 4: Thermodynamic Data of Reaction or Transformation

Reaction or Transformation	Temperature (°C)	Quantity, per mol of atoms (kJ, mol, K)	Comments
1/7 {Fe(γ) + 1/2 O_2(gas) + Al_2O_3(α) → $FeAl_2O_4$(σ)}	750 - 1536	ΔG = –292.800 + 0.0687T	emf [1973Cha]
1/7{$FeAl_2O_4$(σ) → Fe_L + {O}$_{Fe\_L}$ + Al_2O_3(α)}	1550 - 1600	ΔG = 28.01 – 0.01184T	emf [1978Apt]

Reaction or Transformation	Temperature (°C)	Quantity, per mol of atoms (kJ, mol, K)	Comments
$1/2Fe_2O_3+1/2Al_2O_3(\alpha) \rightarrow FeAlO_3(\tau)$	25	$\Delta H = 5.58$	Drop solution calorimetry [2002Maj]
$1/5\{Al_2O_3(\alpha) \rightarrow 2\{Al\}_{Fe\_L} + 3\{O\}_{Fe\_L}\}$	1550 - 1750	$\Delta G = 245.051 - 0.078761T$	Analysis of phase equilibria and emf data [2000Jan]

Table 5: Thermodynamic Properties of Single Phases

Phase	Temperature Range (°C)	Property, per mole of atoms (J, mol, K)	Comment
$FeAl_2O_4$ (σ)	25	$S° = 16.2714$	Adiabatic calorimetry [2003Kle]
$FeAl_2O_4$ (σ)	25 26.85 46.85 66.85 86.85 106.85 130.67	$C_p = 17.7714$ $C_p = 17.8286$ $C_p = 18.5286$ $C_p = 19.1571$ $C_p = 19.7$ $C_p = 20.2$ $C_p = 20.7143$	Adiabatic calorimetry [2003Kle]
$FeAlO_3$ (τ)	25 - 1277	$C_p = 35.16 - 0.0004944 \cdot T - 3.916 \cdot 10^5/T^2 - 183.46/T^{0.5} + 1.5092 \cdot 10^{-6} \cdot T^2$	Differential scanning calorimetry [2002Maj]

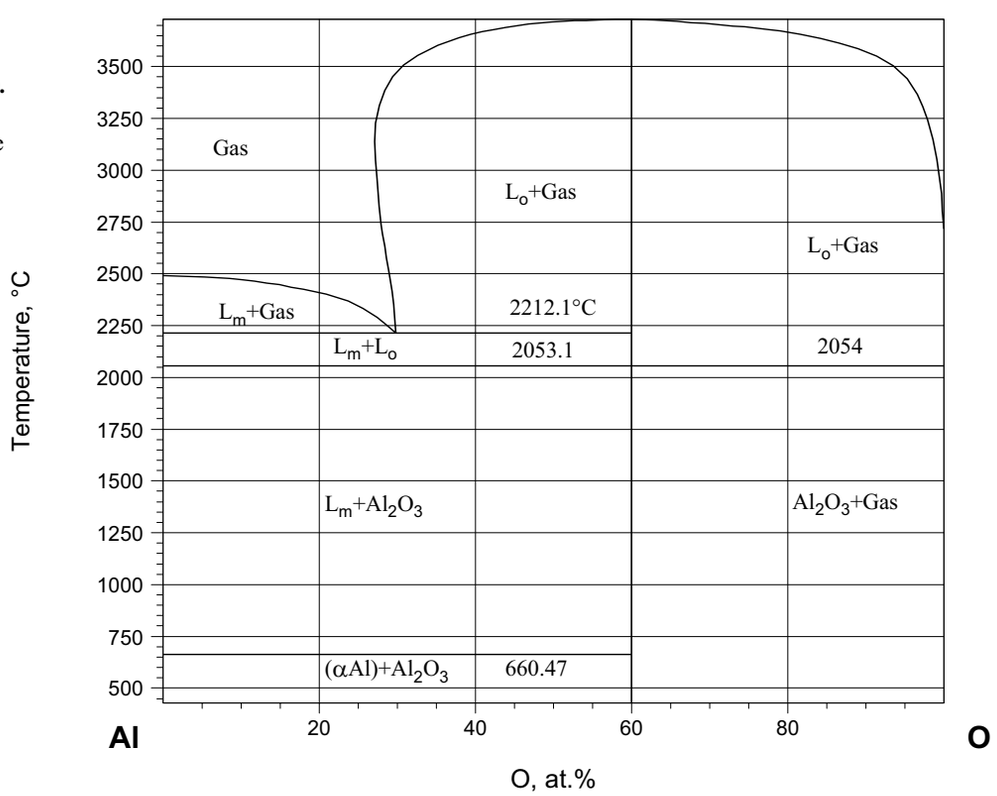

Fig. 1a: Al-Fe-O. Temperature – composition phase diagram of the Al-O system

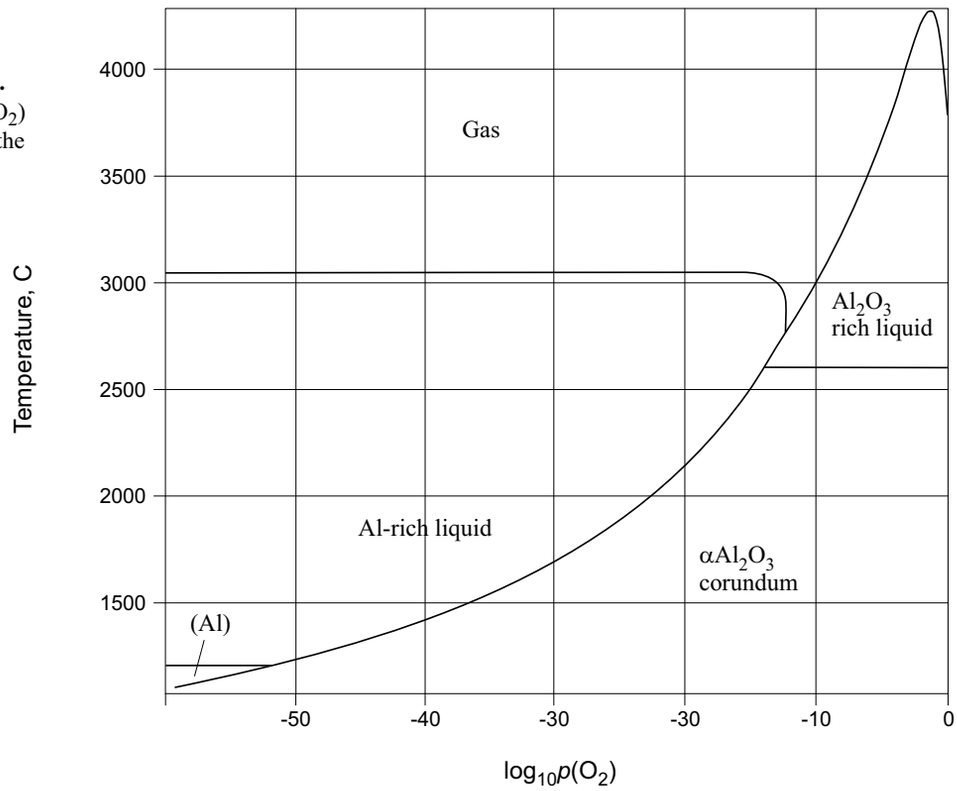

Fig. 1b: Al-Fe-O. Temperature – $p(O_2)$ phase diagram of the Al-O system

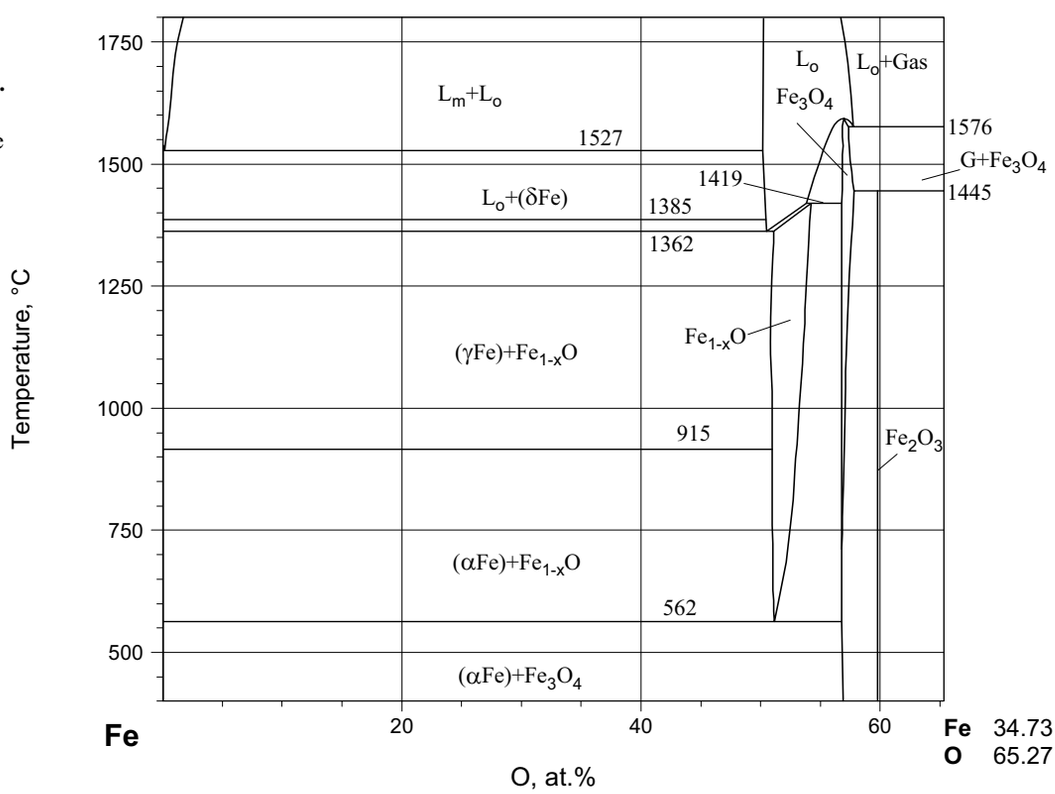

Fig. 2a: Al-Fe-O. Temperature – composition phase diagram of the Fe-O system

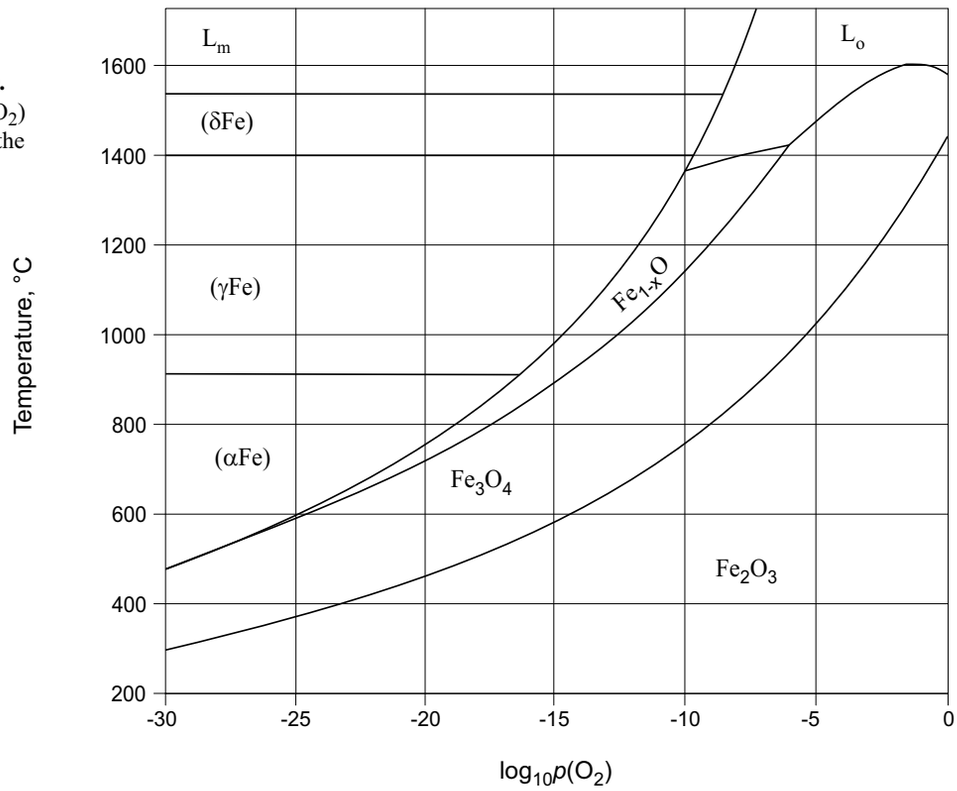

Fig. 2b: Al-Fe-O. Temperature – $p(O_2)$ phase diagram of the Fe-O system

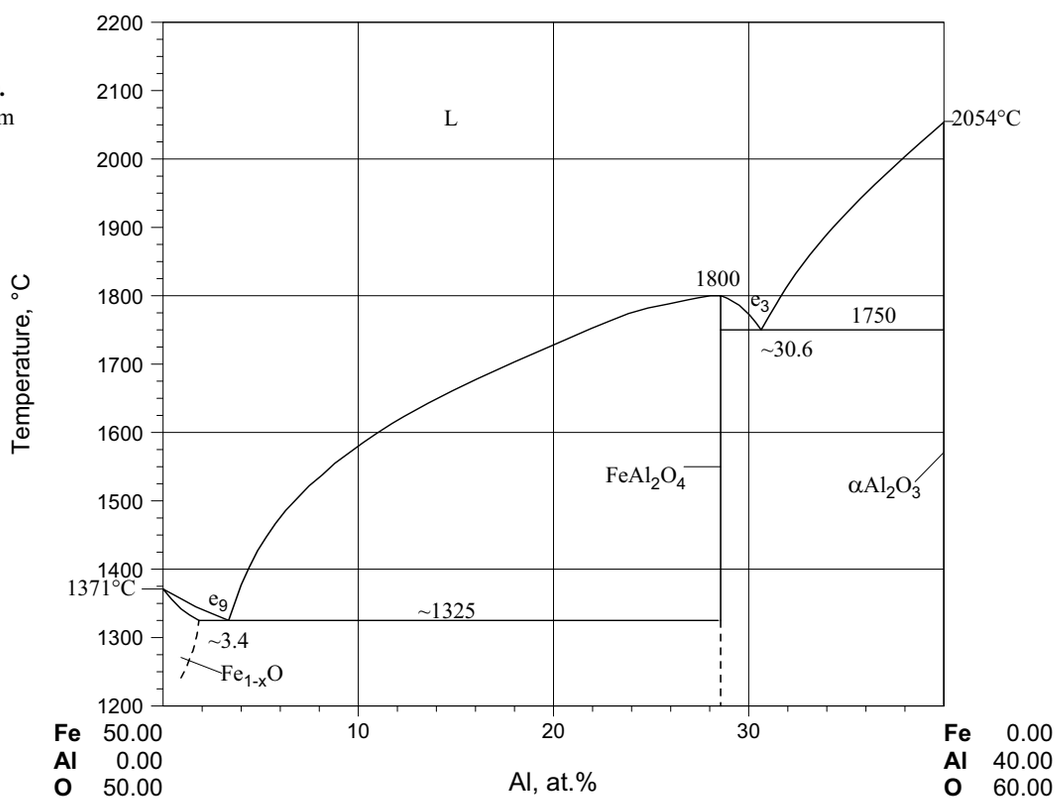

Fig. 3: Al-Fe-O. Quasibinary system $FeO\text{-}Al_2O_3$

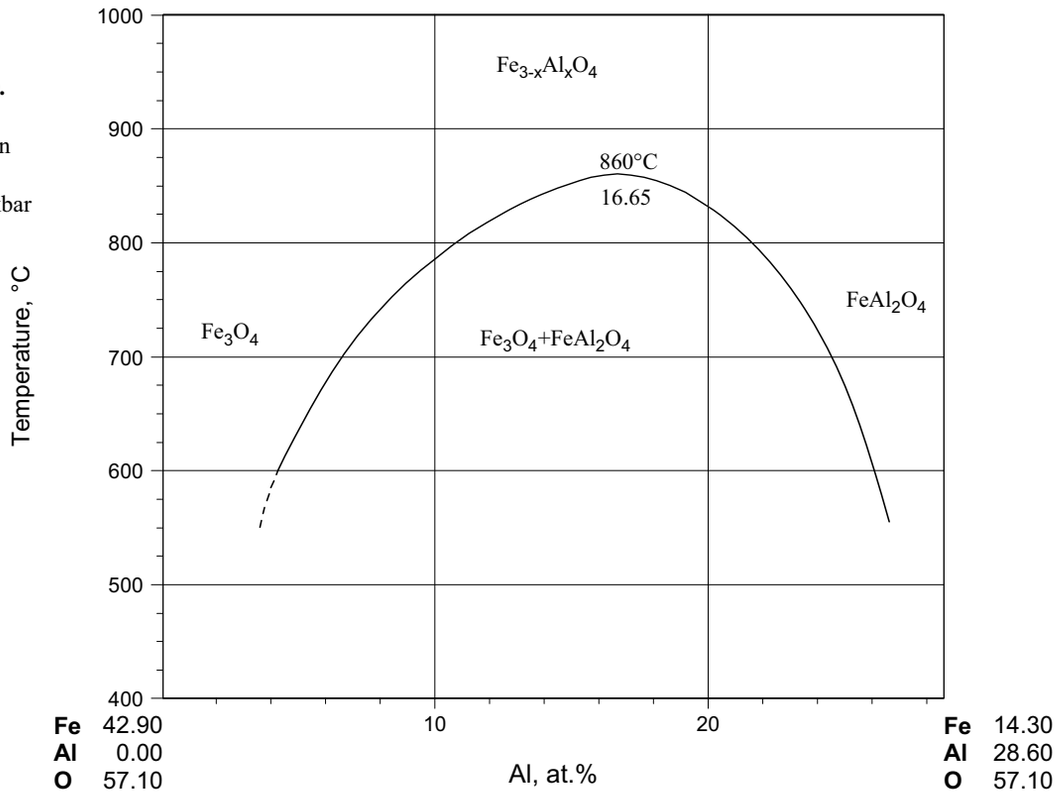

Fig. 4: Al-Fe-O. Subsolidus quasibinary section Fe_3O_4-$FeAl_2O_4$ under pressure 2 kbar

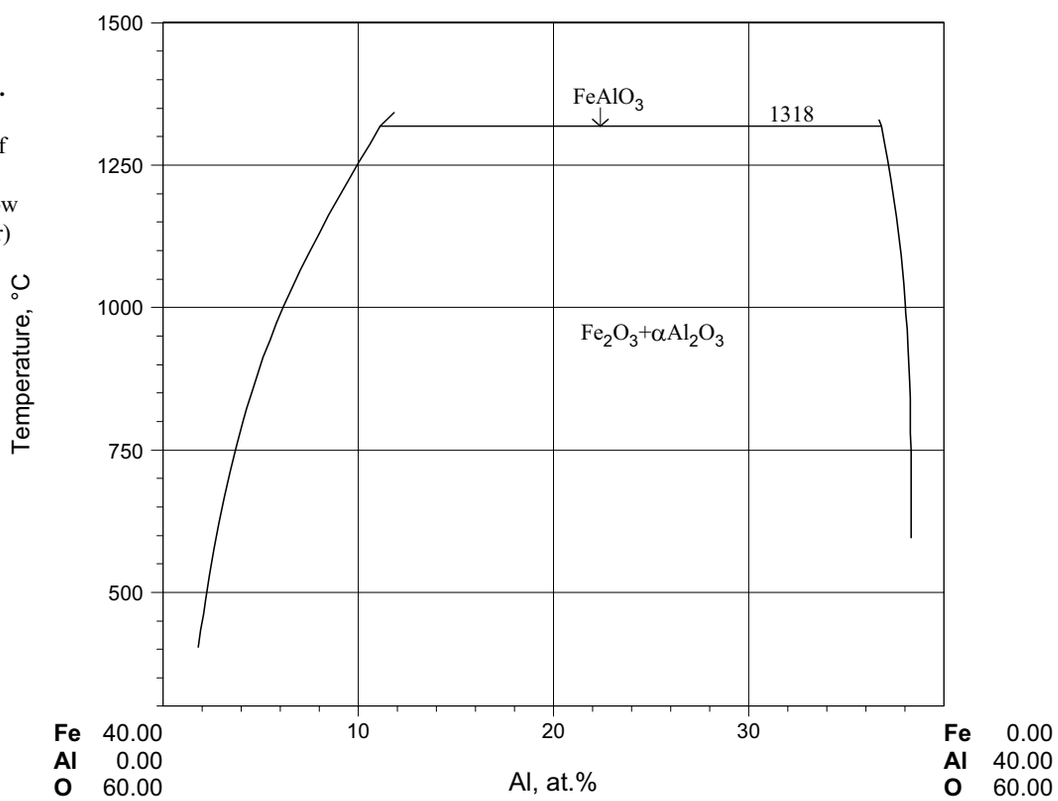

Fig. 5: Al-Fe-O. Subsolidus quasibinary part of the section Fe_2O_3-Al_2O_3 below 1350°C (1.013 bar)

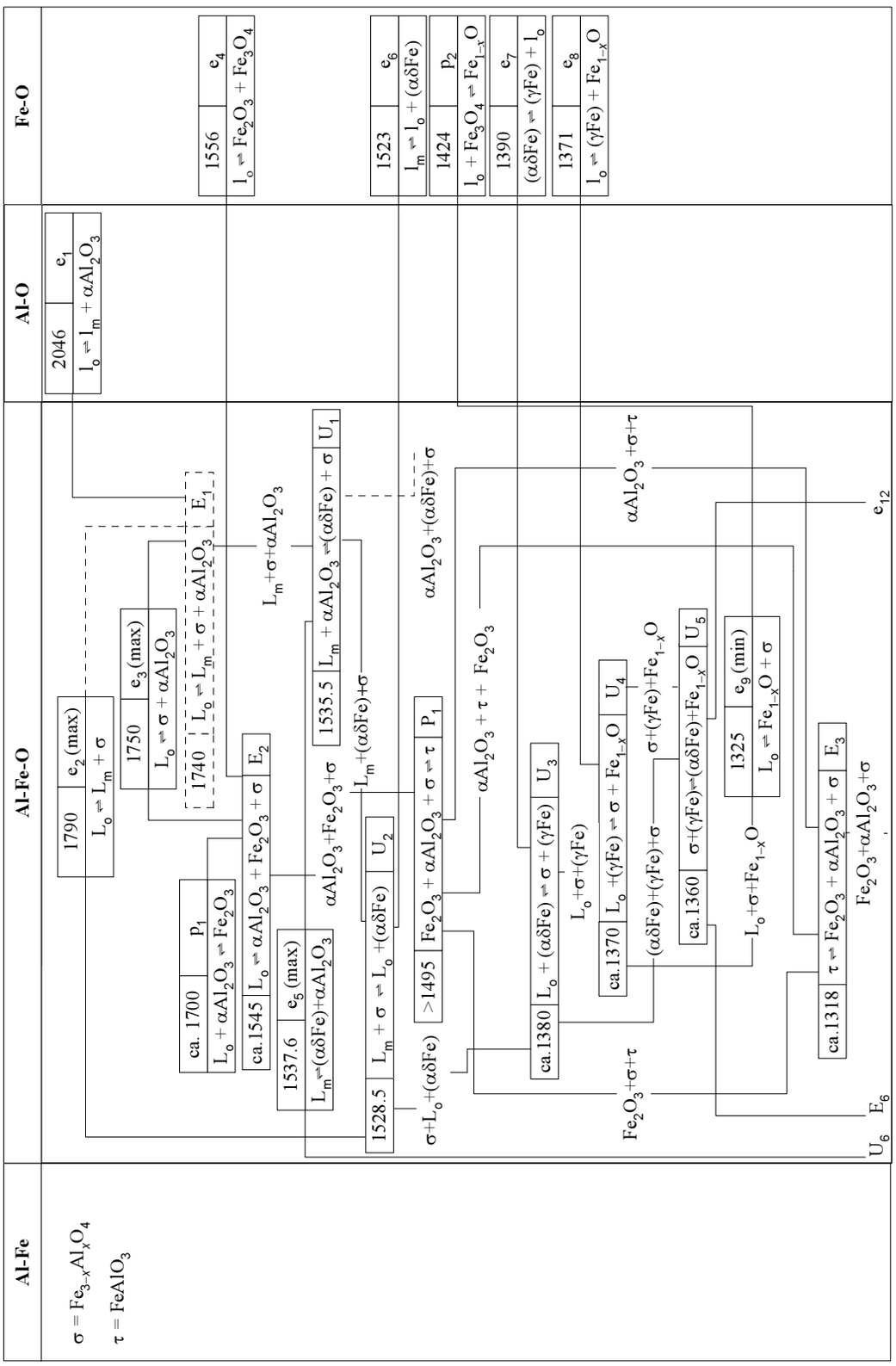

Fig. 6a: Al-Fe-O. Reaction scheme, part 1

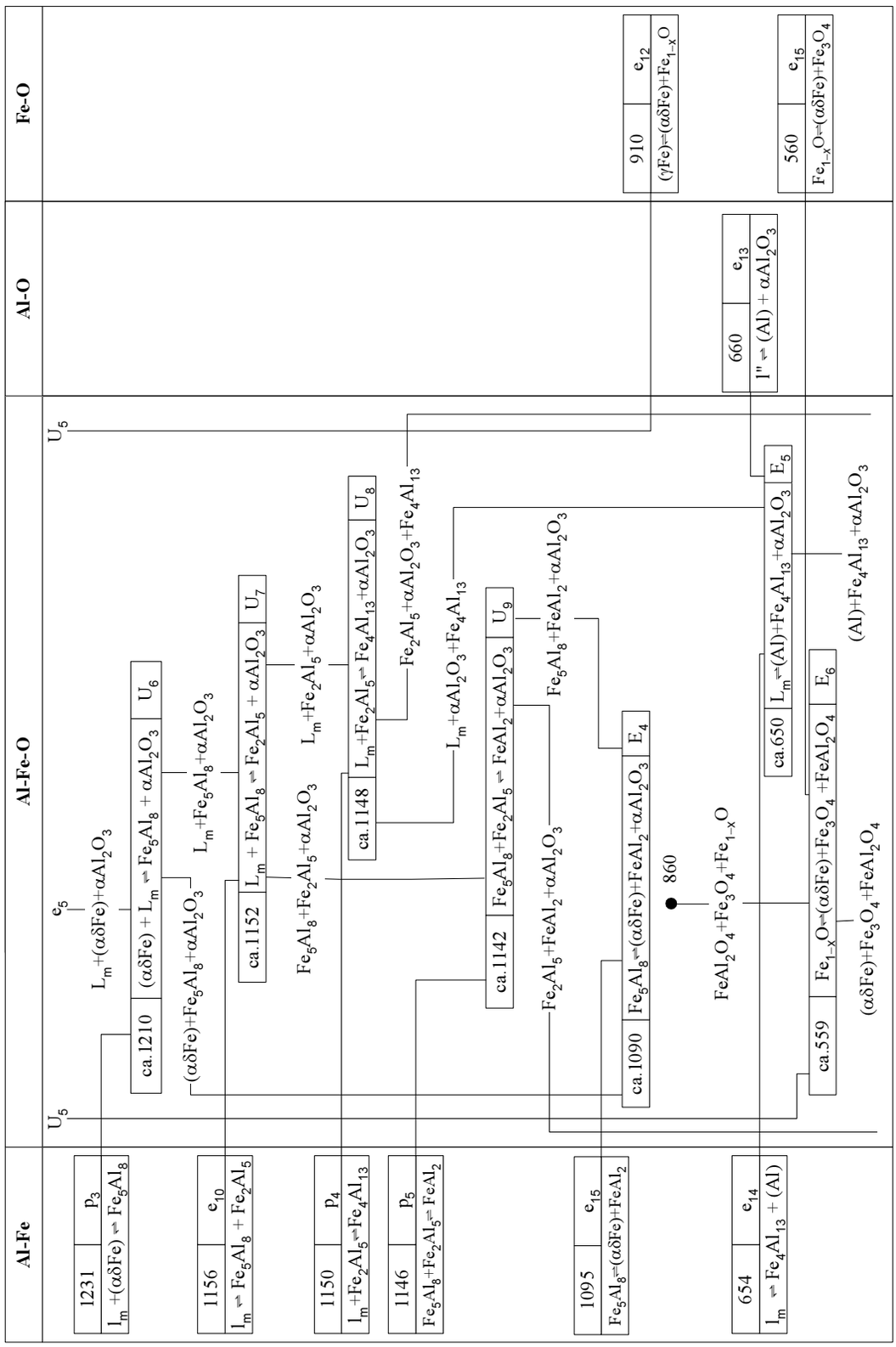

Fig. 6b: Al-Fe-O. Reaction scheme, part 2

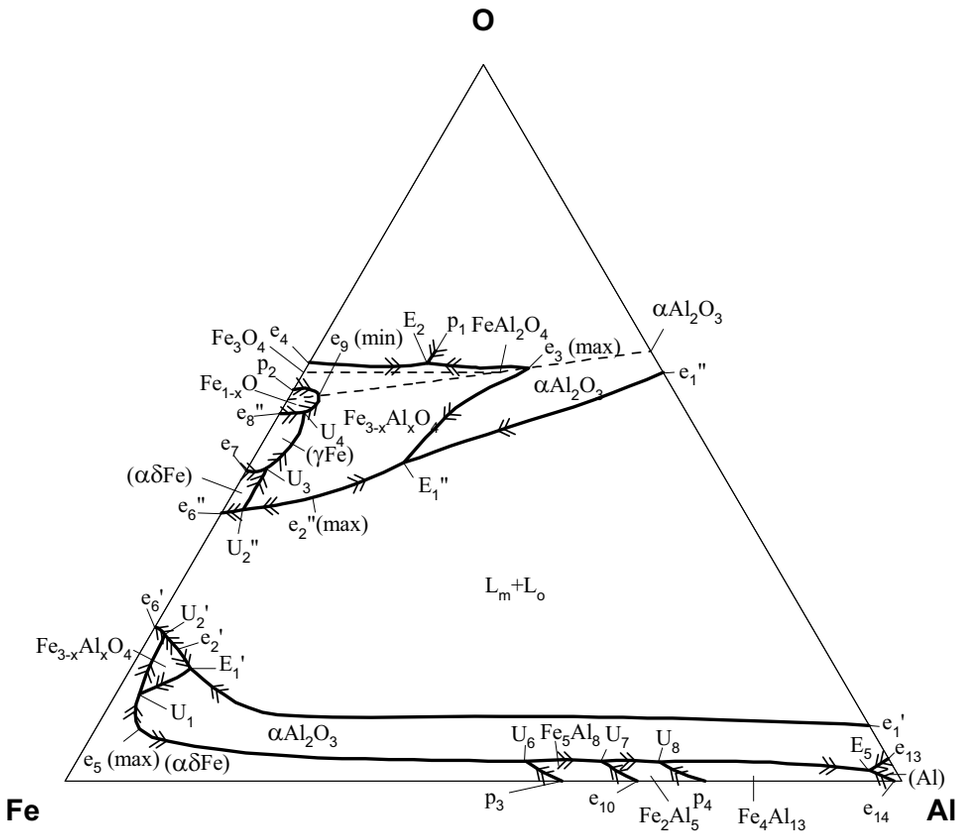

Fig. 7: Al-Fe-O. Schematic liquidus surface of Fe-Fe_2O_3-Al_2O_3-Al region under pressure, no gas equilibria

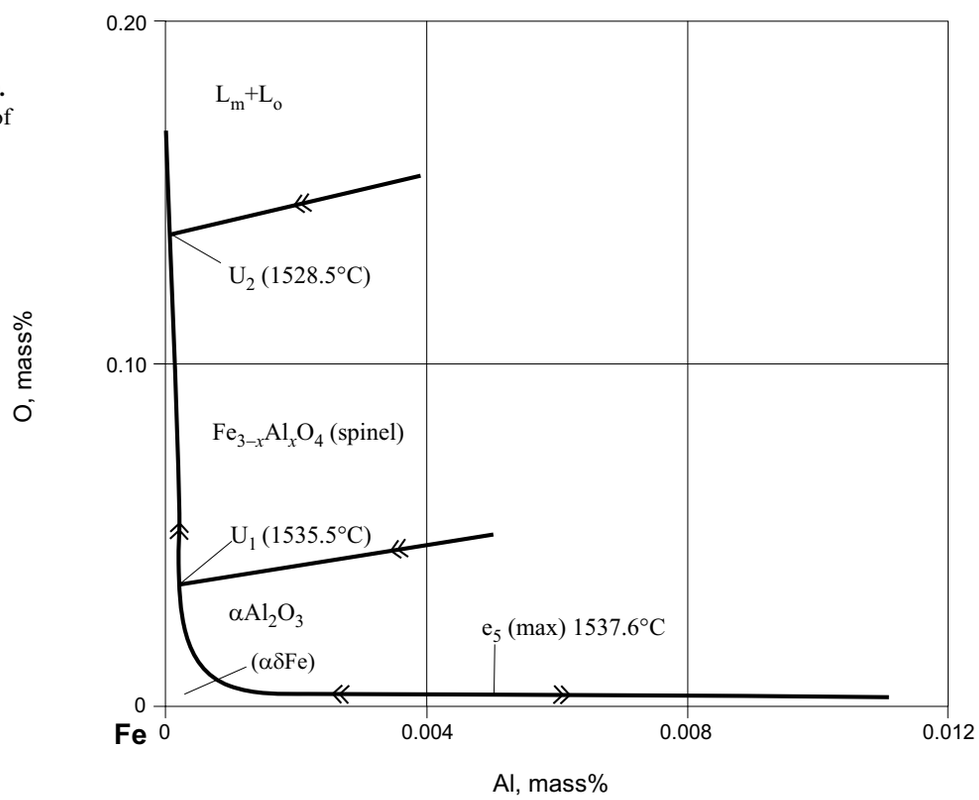

Fig. 8: Al-Fe-O. Liquidus surface of the Fe corner

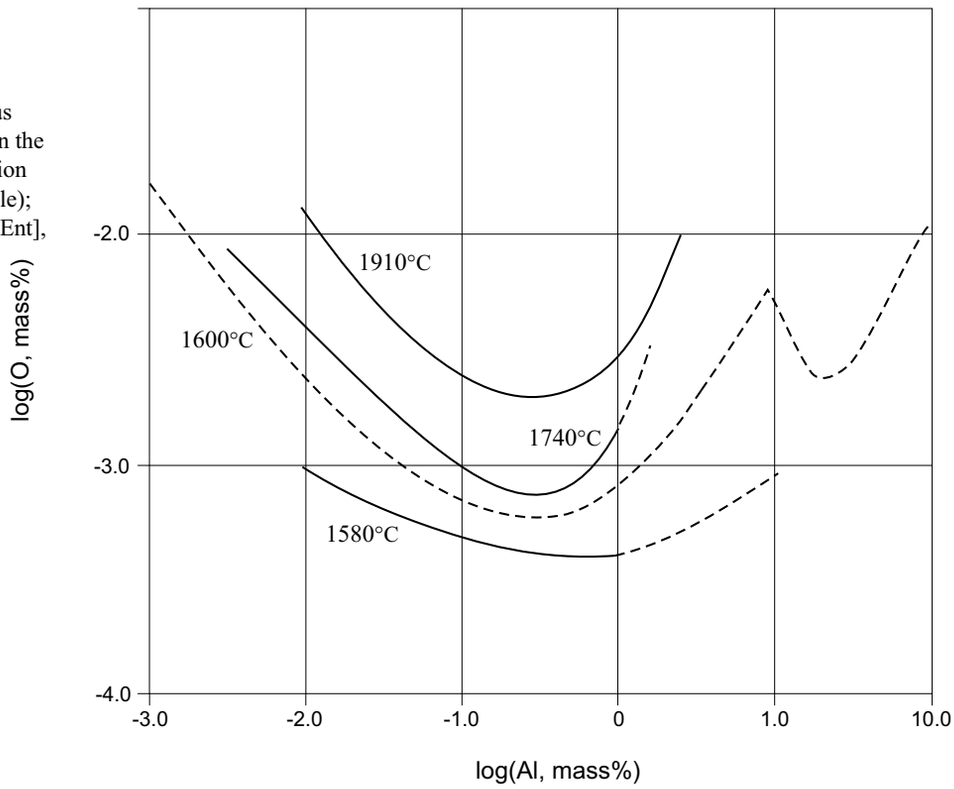

Fig. 9: Al-Fe-O. Isotherms of liquidus surface of αAl_2O_3 in the Fe corner (deoxidation equilibrium, log scale); 1740, 1910°C [1963Ent], 1600°C [1981She], 1580°C [1967Swi]

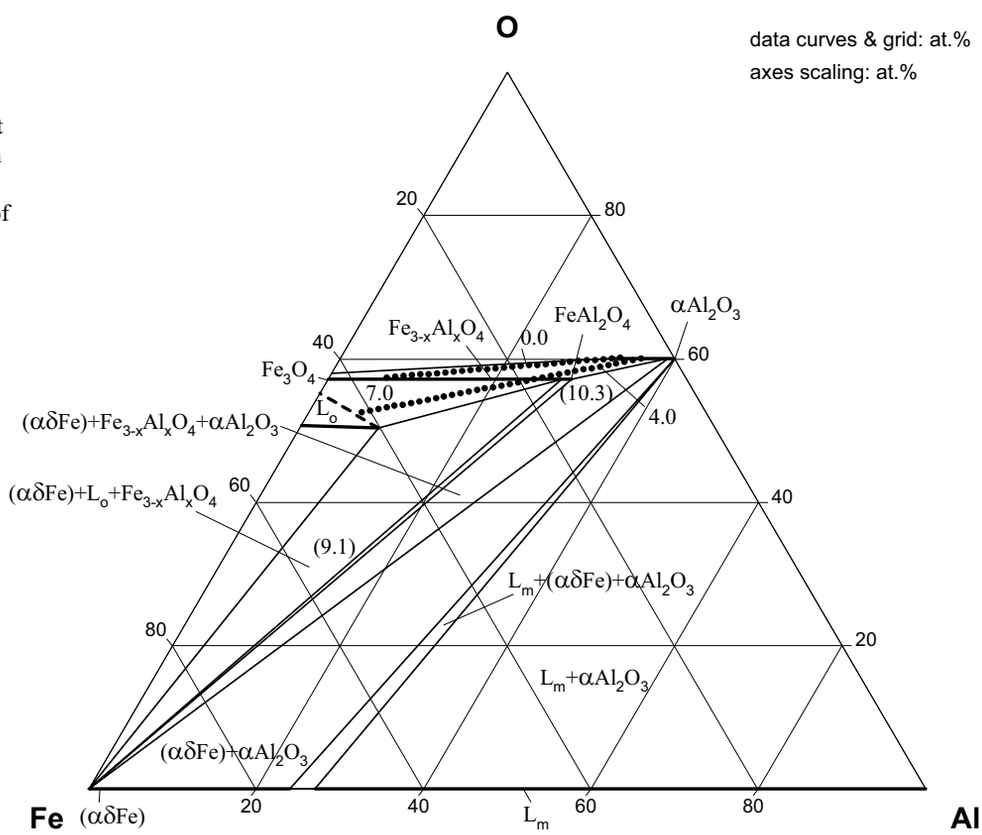

Fig. 10: Al-Fe-O. Isothermal section at 1500°C. Numbers in tie-triangles and on tie-lines are values of $-\log p(O_2)$(bar)

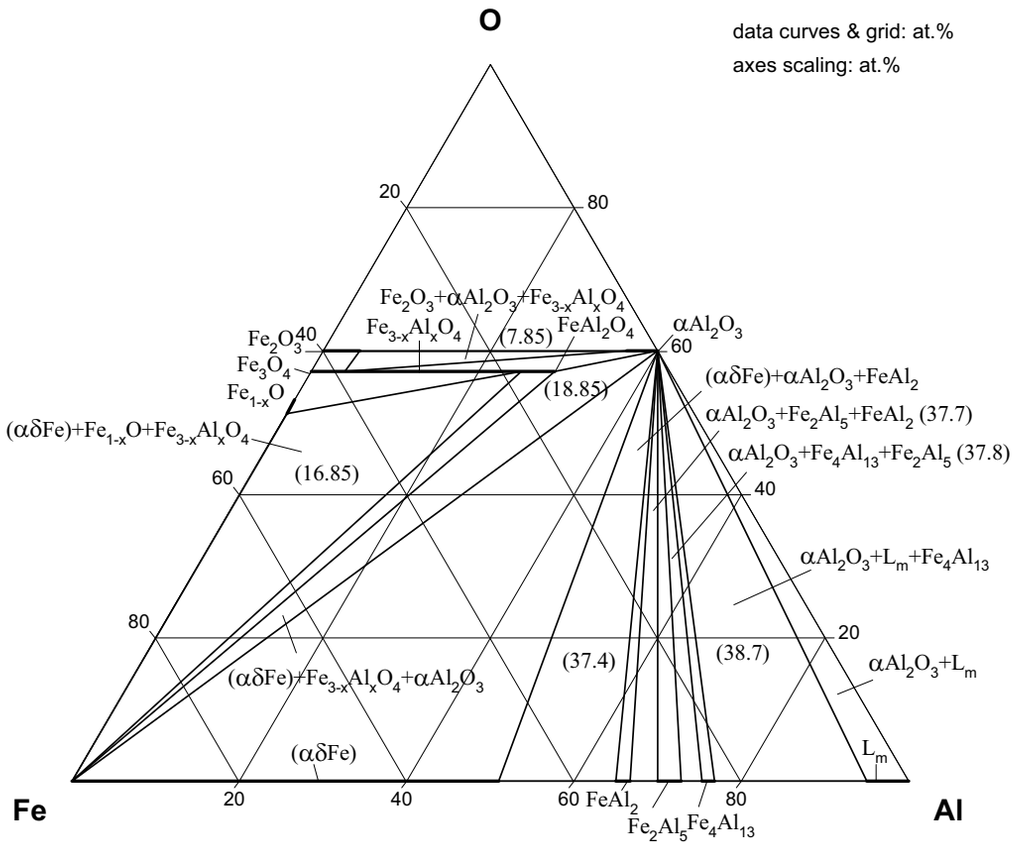

Fig. 11: Al-Fe-O. Isothermal section at 900°C. Numbers in tie-triangles and on tie-lines are values of $-\log p(O_2)$(bar).

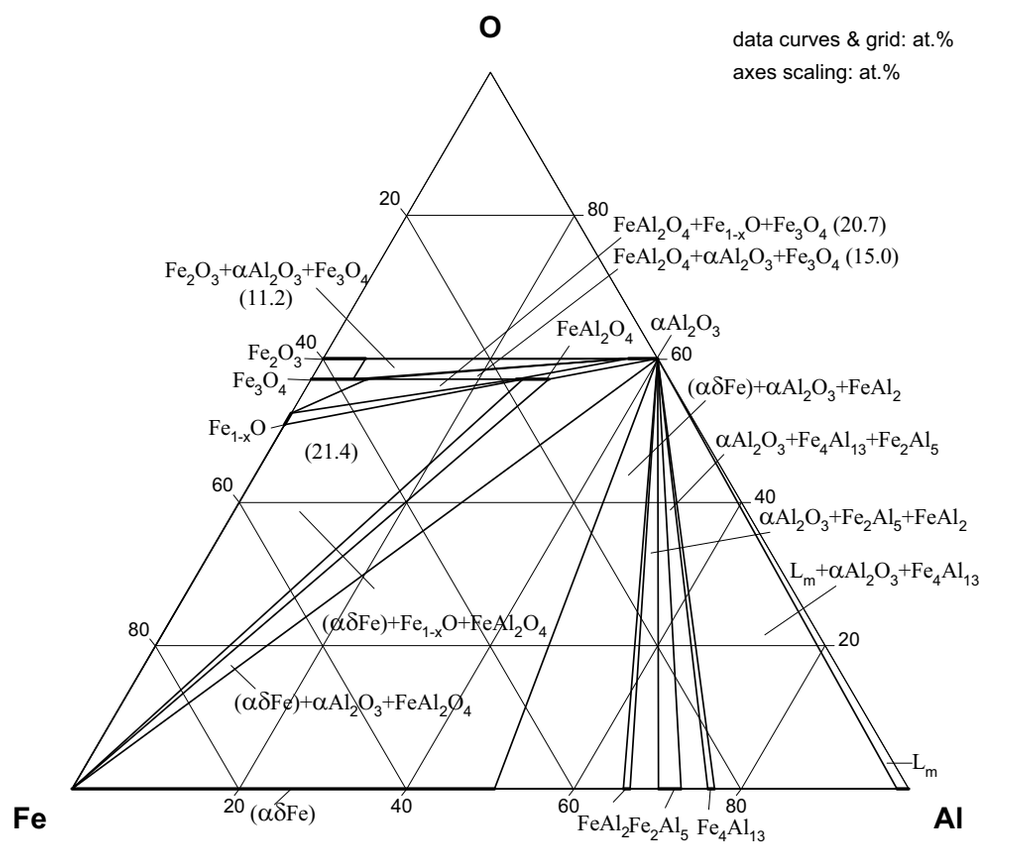

Fig. 12: Al-Fe-O. Isothermal section at 700°C

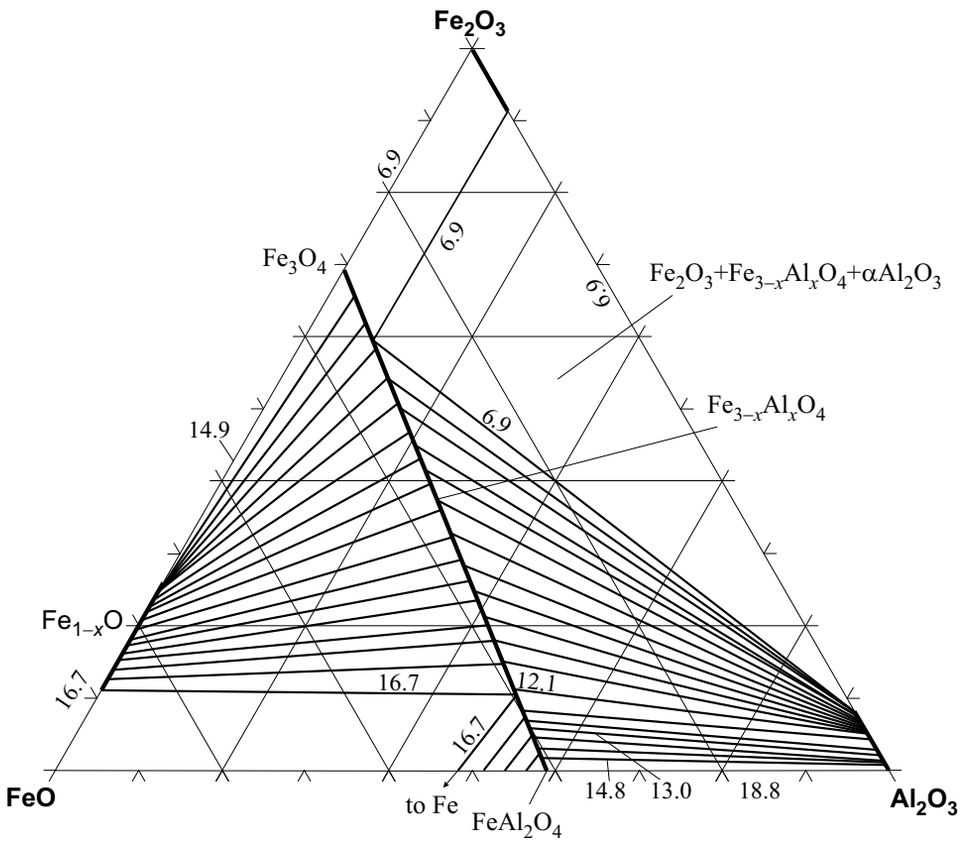

Fig. 13: Al-Fe-O. Isothermal section at 900°C (Numbers in tie-triangles and are values of log $p(O_2)$(bar)). Concentrations are given in mass percent.

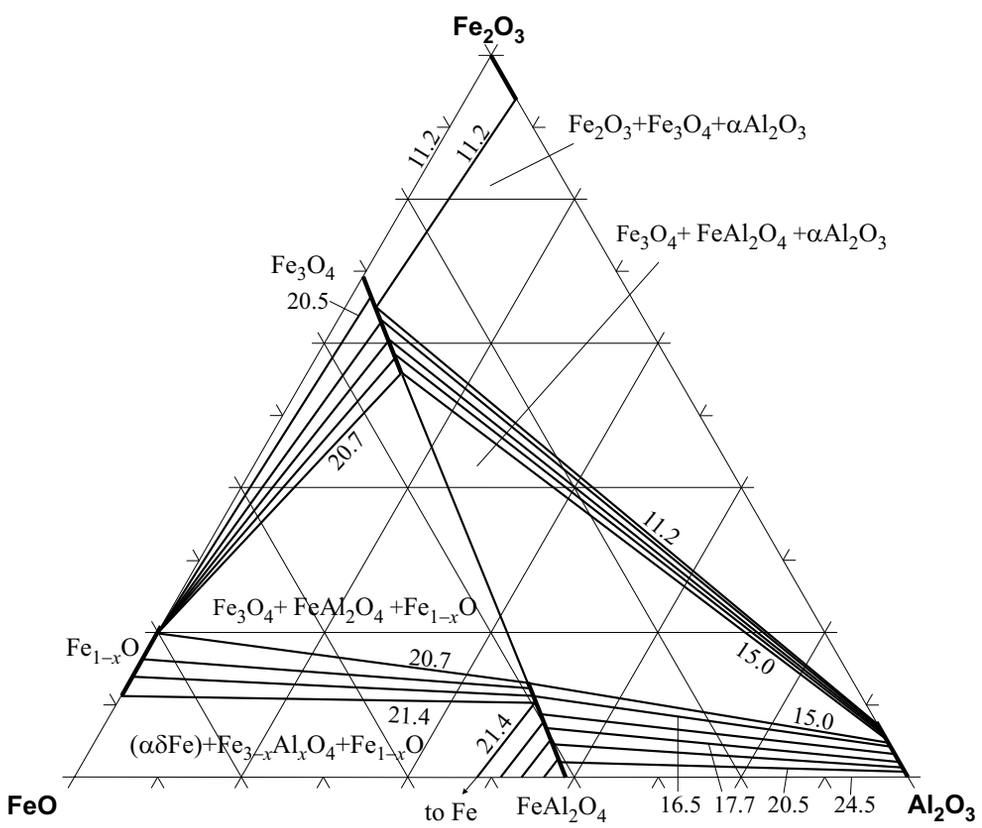

Fig. 14: Al-Fe-O. Isothermal section of the partial FeO-Fe_2O_3-Al O system at 700°C. Numbers in tie-triangles and on tie-lines are equilibrium values of log $p(O_2)$(bar)). Concentrations are given in mass percent.

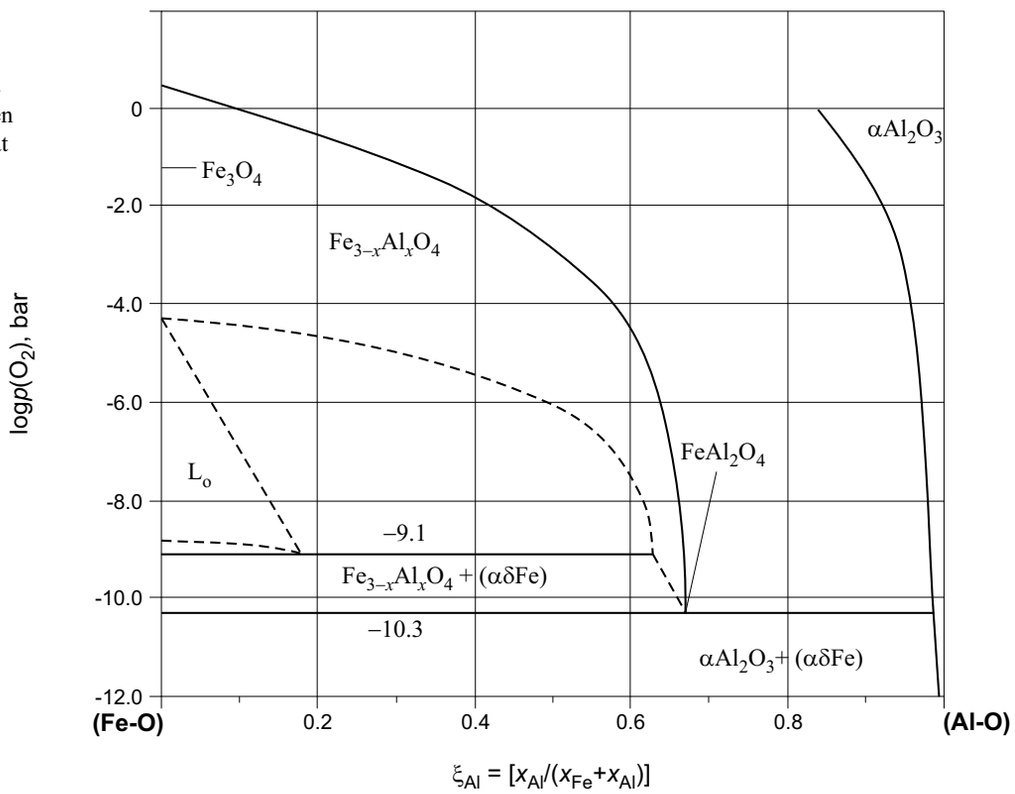

Fig. 15: Al-Fe-O. Equilibrium oxygen pressure diagram at 1500°C

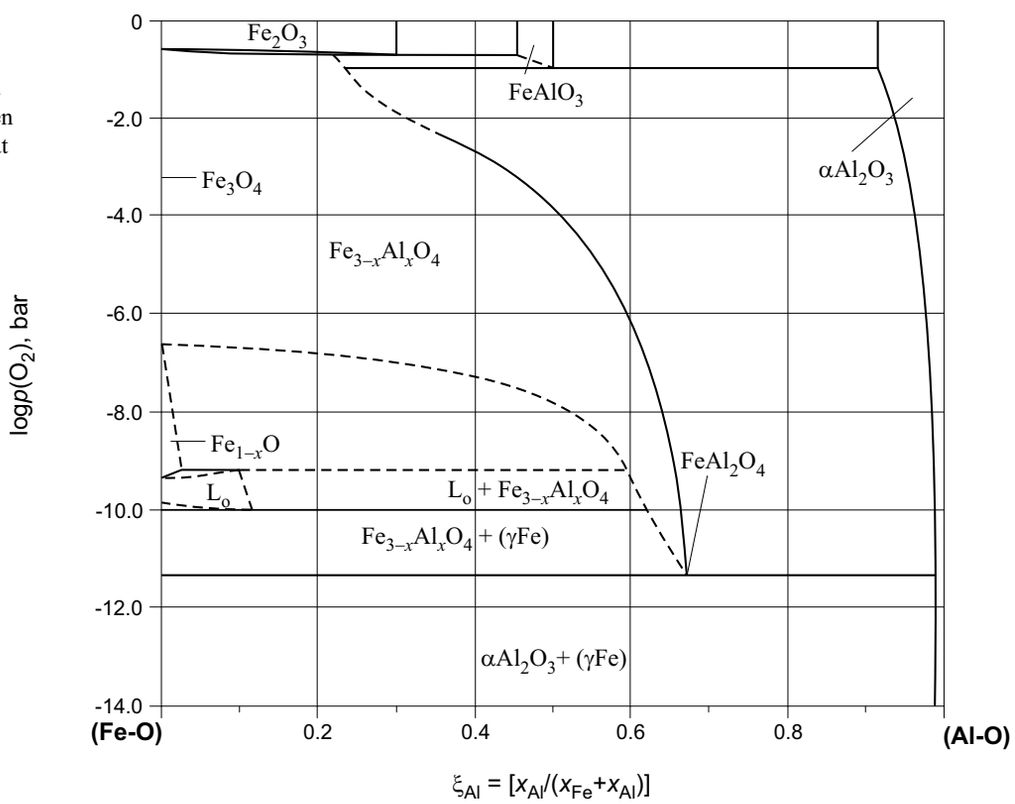

Fig. 16: Al-Fe-O. Equilibrium oxygen pressure diagram at 1380°C

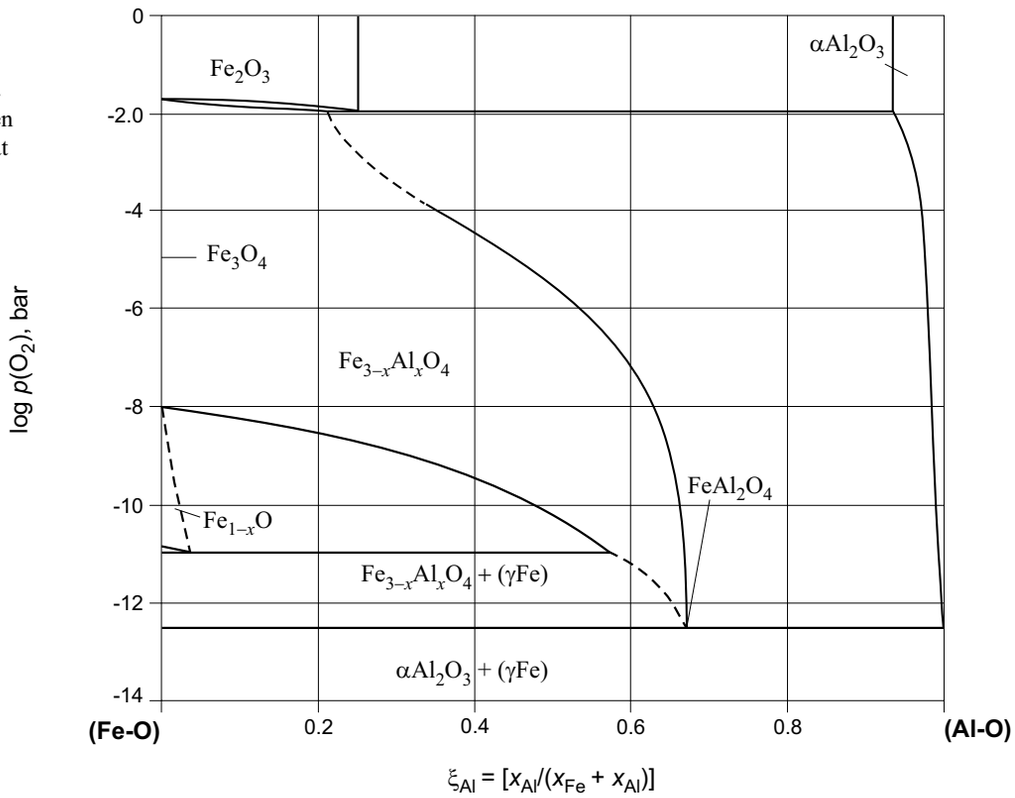

Fig. 17: Al-Fe-O. Equilibrium oxygen pressure diagram at 1280°C

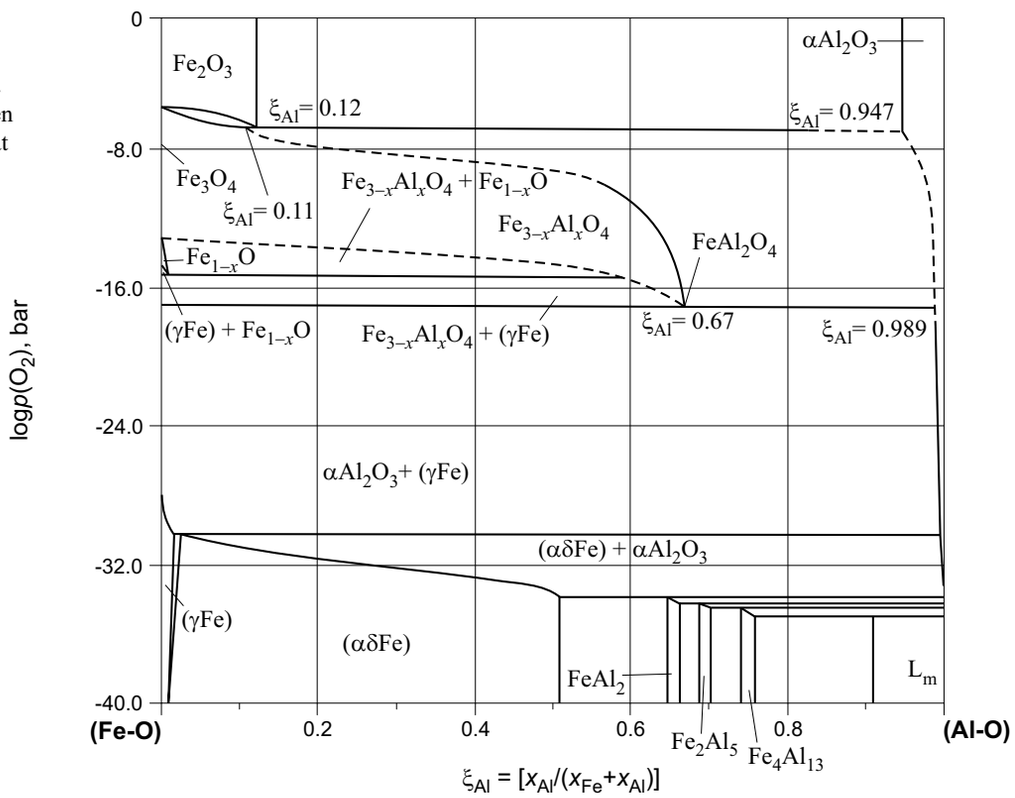

Fig. 18: Al-Fe-O. Equilibrium oxygen pressure diagram at 1000°C

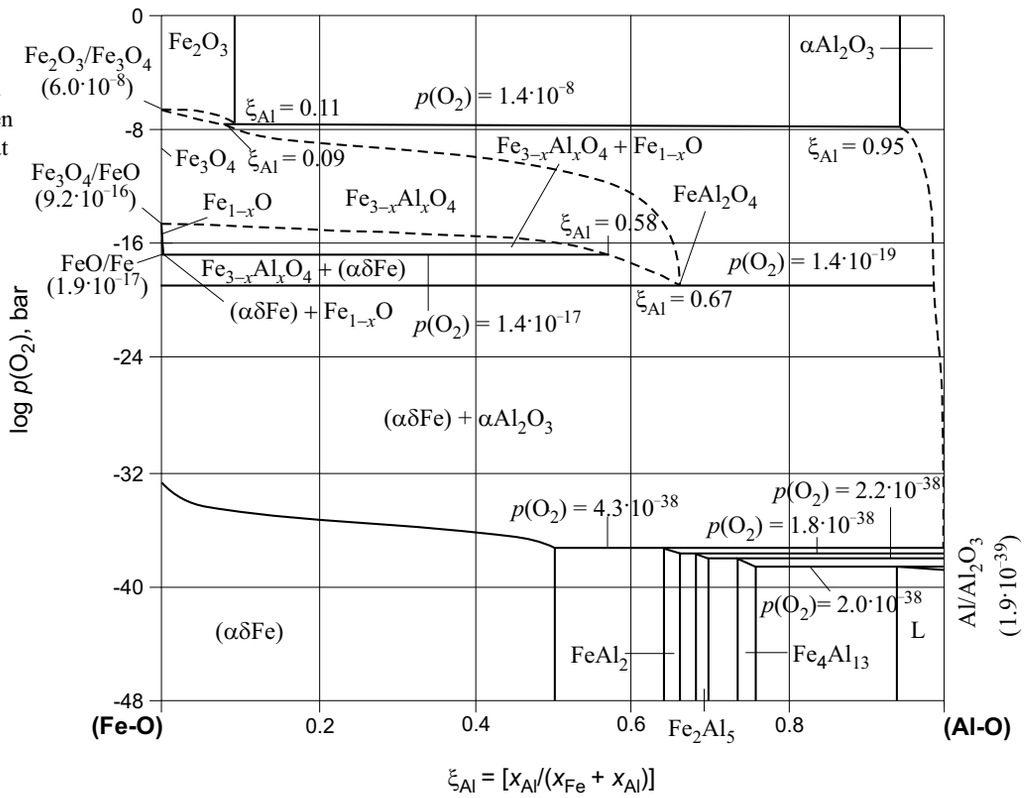

Fig. 19: Al-Fe-O. Equilibrium oxygen pressure diagram at 900°C

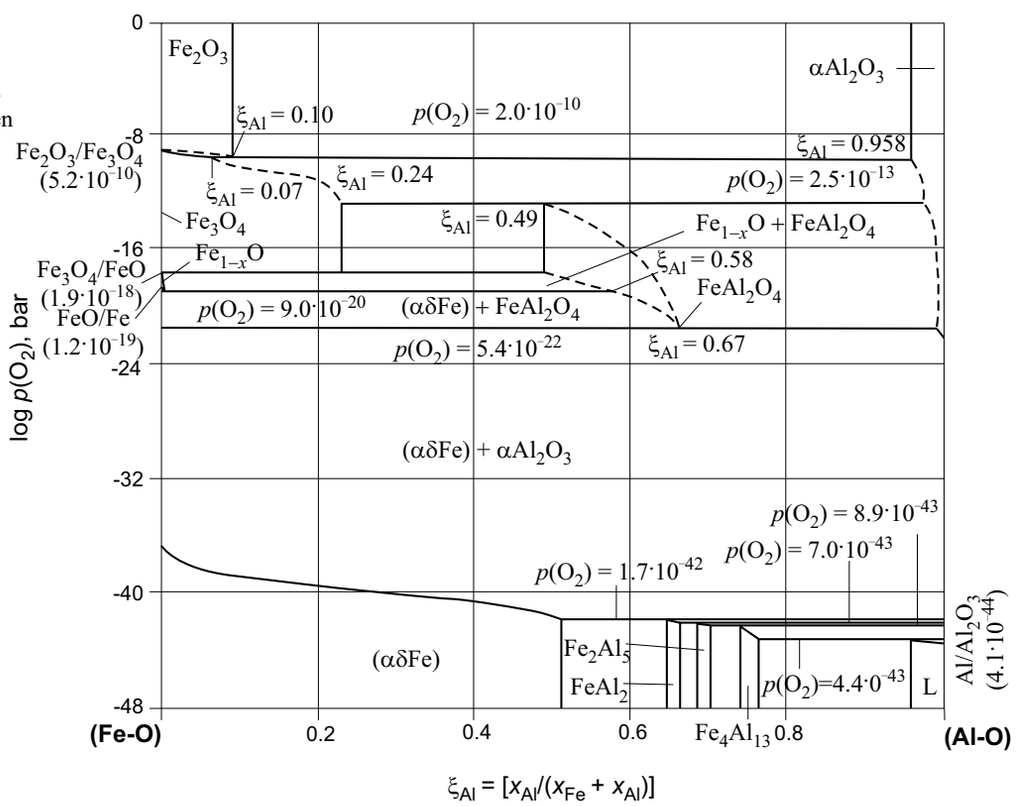

Fig. 20: Al-Fe-O. Equilibrium oxygen pressure diagram at 800°C

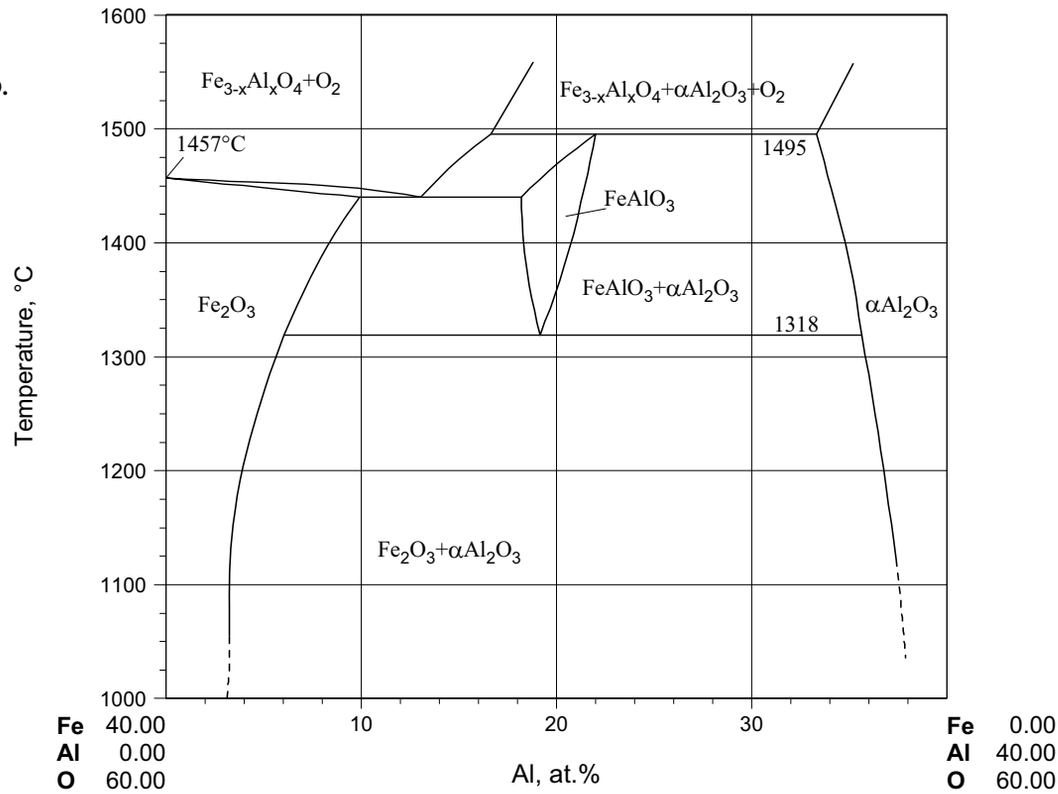

Fig. 21: Al-Fe-O. Vertical section Fe_2O_3-Al_2O_3 at $p(O_2)$ =1 bar

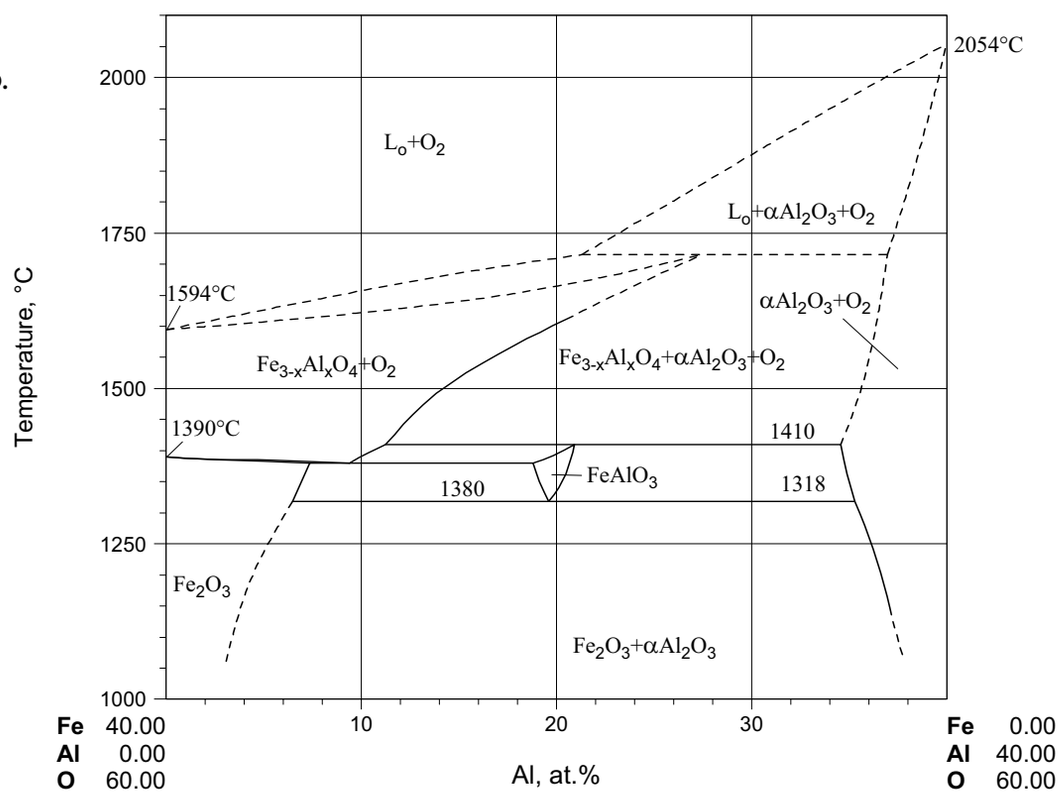

Fig. 22: Al-Fe-O. Vertical section Fe_2O_3-Al_2O_3 at $p(O_2)$ = 0.21 bar

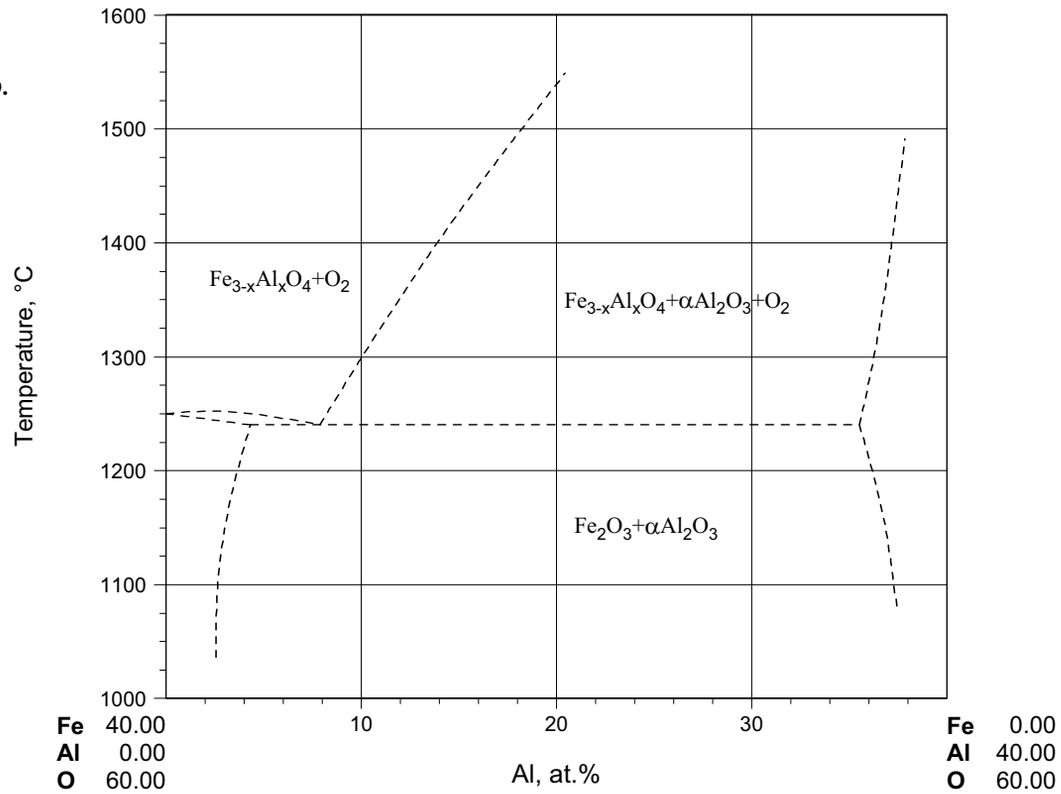

Fig. 23: Al-Fe-O. Vertical section Fe_2O_3-Al_2O_3 at $p(O_2) < 0.03$ bar

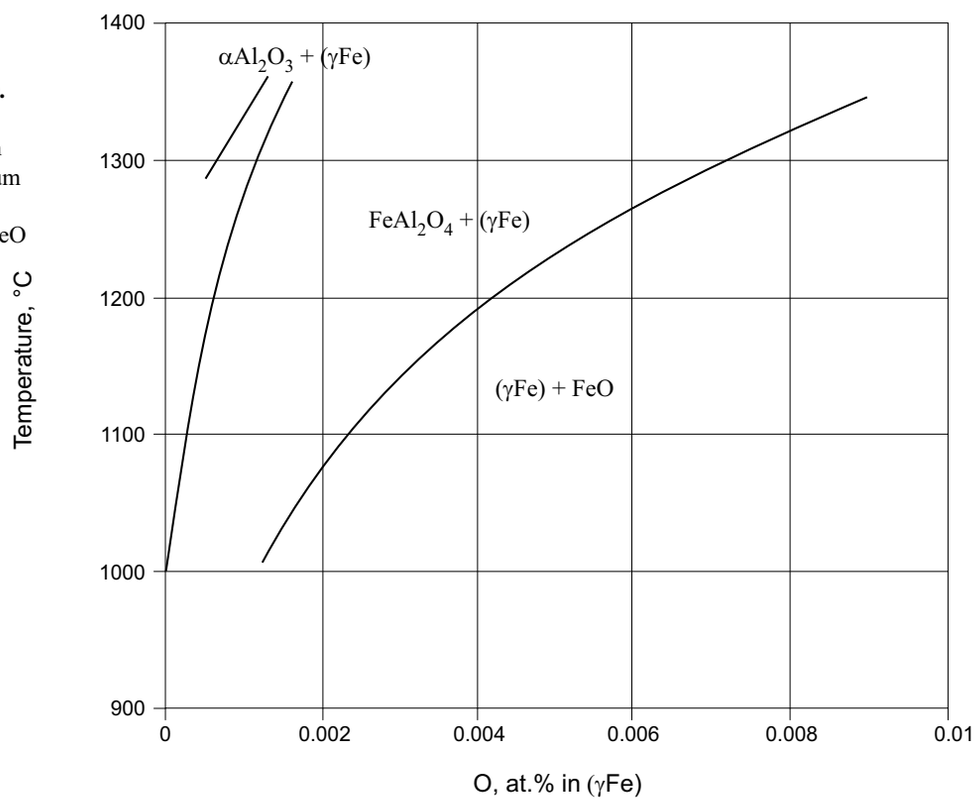

Fig. 24: Al-Fe-O. Stability diagram. Oxygen content in (γFe) in equilibrium with αAl_2O_3, $FeAl_2O_4(\sigma)$ and FeO

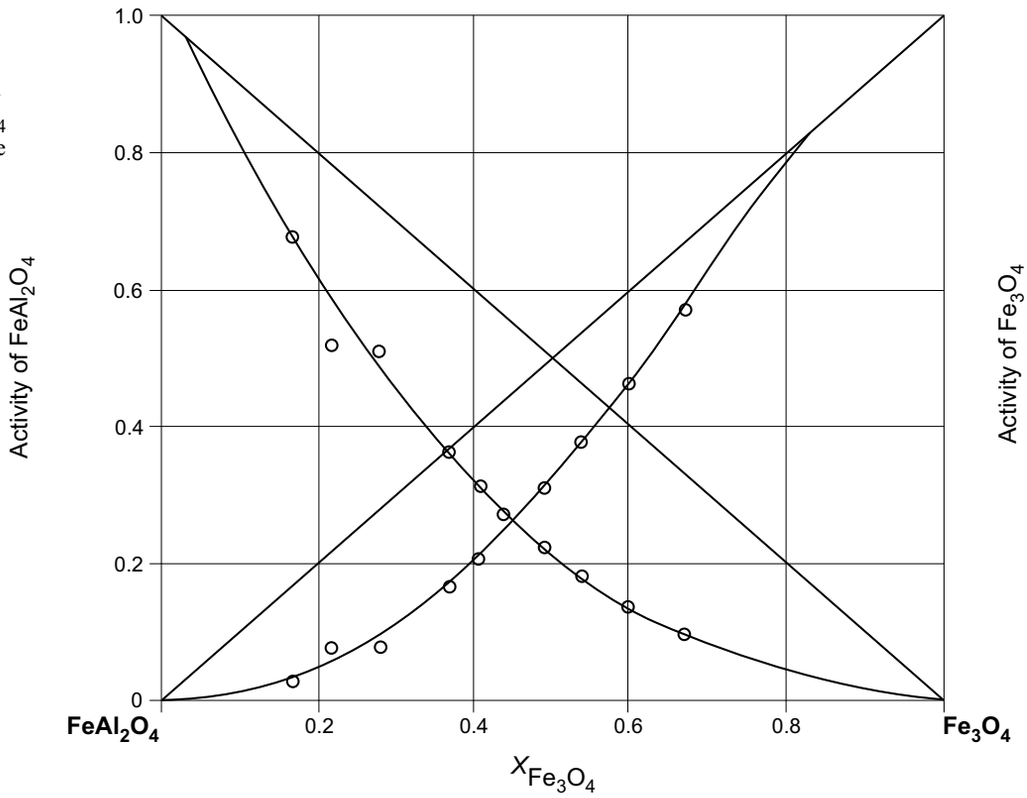

Fig. 25: Al-Fe-O. Activities of Fe_3O_4 and $FeAl_2O_4$ in the Fe_3O_4-$FeAl_2O_4$ system at 900°C

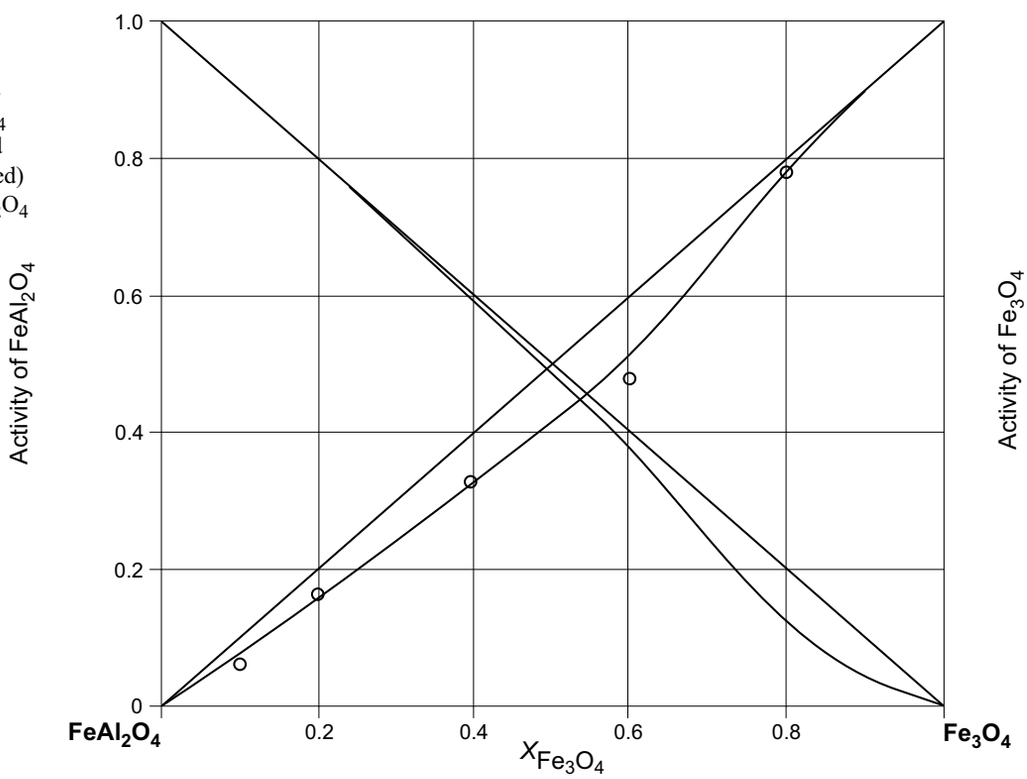

Fig. 26: Al-Fe-O. Activities of Fe_3O_4 (experimental) and $FeAl_2O_4$ (calculated) in the Fe_3O_4-$FeAl_2O_4$ system at 1300°C

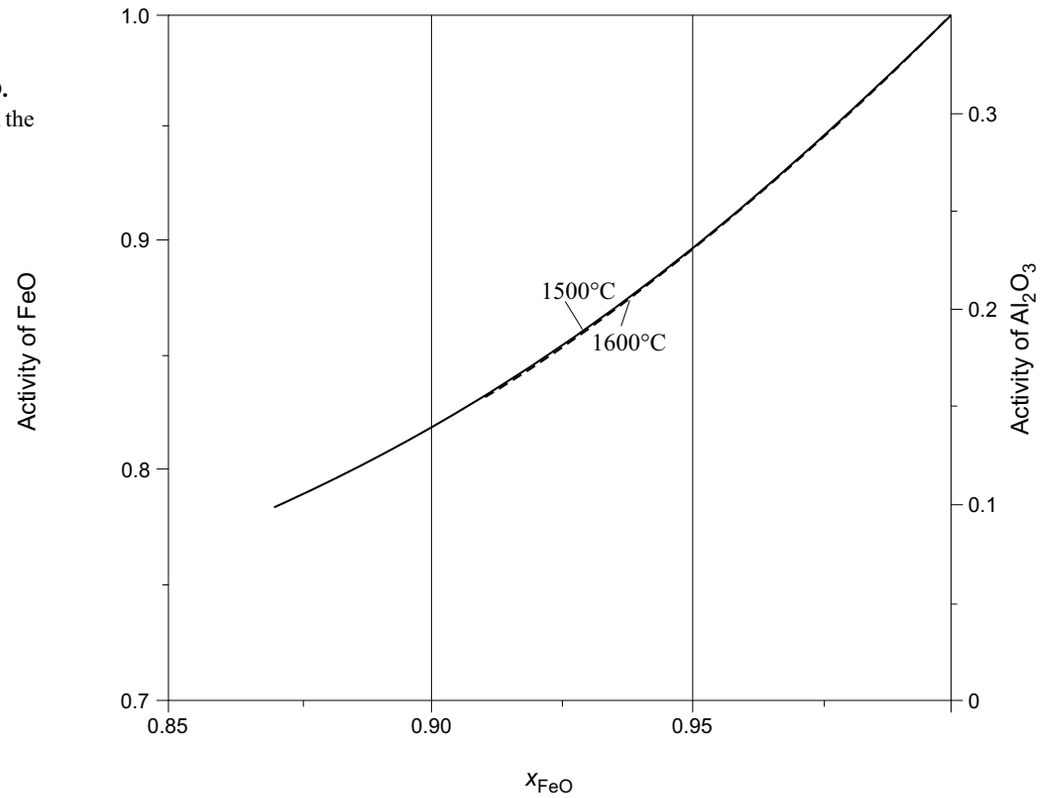

Fig. 27: Al-Fe-O. Activity of FeO in the $FeO\text{-}Al_2O_3$ liquid phase

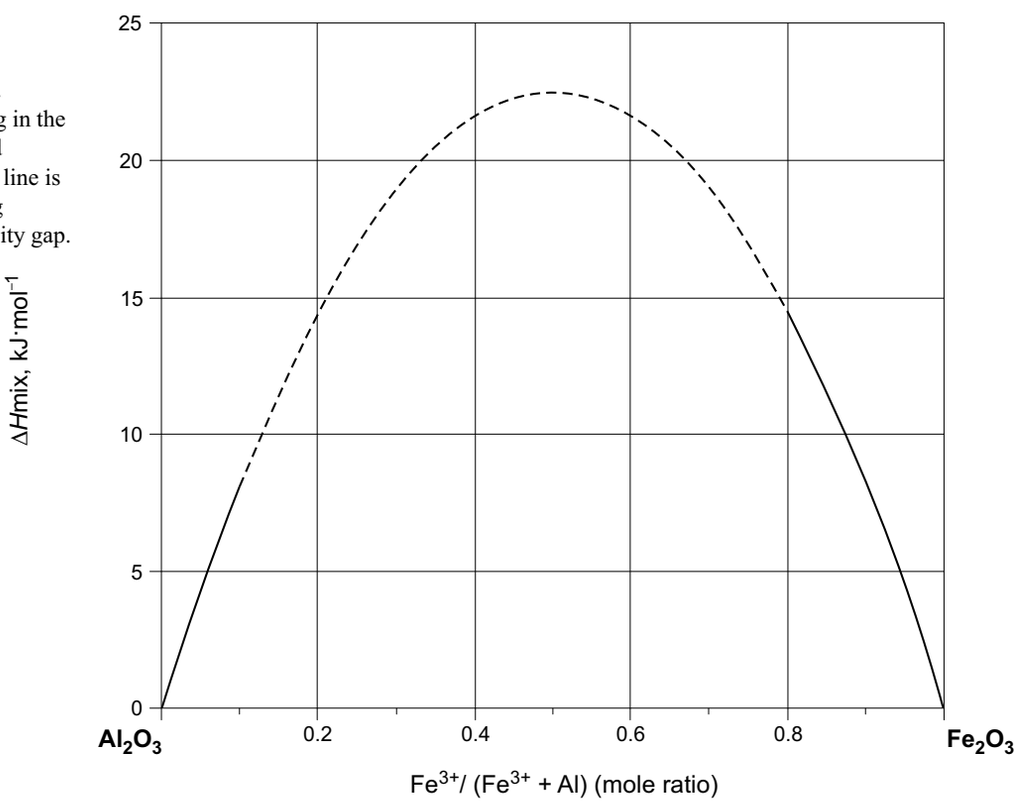

Fig. 28: Al-Fe-O. Enthalpy of mixing in the $Fe_2O_3\text{-}Al_2O_3$ solid solution. The dash line is enthalpy of mixing within the miscibility gap.

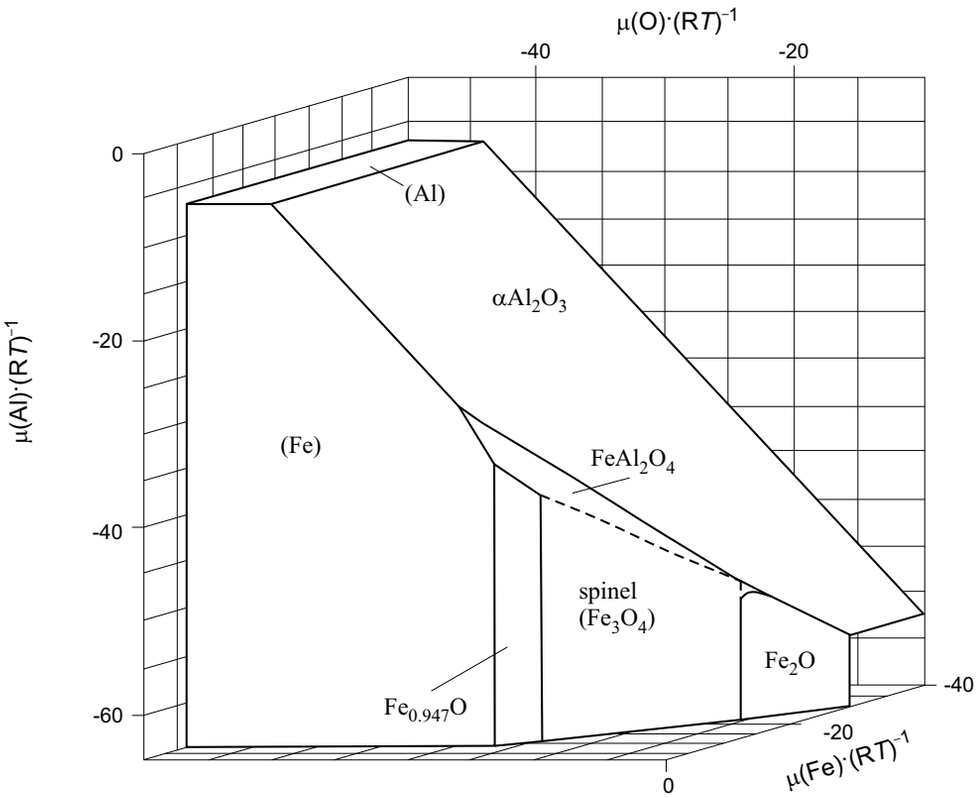

Fig. 29: Al-Fe-O. Chemical potential phase diagram at 1300°C. The spinel phase is treated as ideal solution. The case when Fe_3O_4 and $FeAl_2O_4$ are treated as different phases is shown by a dashed line.